A Full Digital MAPS Based Electromagnetic Calorimeter and its Applications

Hongkai Wang

Nuclear and Radiation Safety Center, MEE

Utrecht University

Outline

- Introduction （Physics motivation, detector upgrade…）
- Design (Construction, measurement setup, electronics…)
- Raw Data Quality (Challenges…)
- Test Beam Data Analysis (Solutions of challenges…)
- Simulation (Charge sharing, noise …)
- Results (Linearity, energy & position resolution, shower profile…)
- Other Application （Proton CT）
- Conclusions

EM Calorimeter in particle physics

Electromagnetic shower

- When a photon / electron / positron enters in thick layers of material, secondary e and gamma's re-interact, thus leading to the production of showers.
- **Dominant processes at high energies (E > 1 GeV) :** Photons : Pair production Electrons : Bremsstrahlung

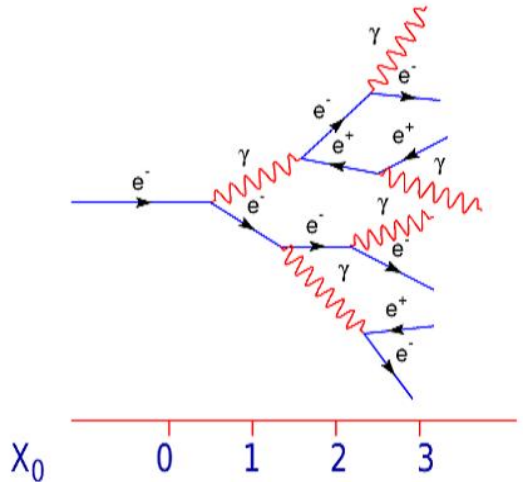

Electromagnetic Calorimeter (EMCal)

- Classified according to construction technique into sampling and homogeneous calorimeters.
- Shower development in longitudinal direction is governed by X_0.

  e⁻ loses [1 - 1/e] = 63% of energy in 1 Xo (Brems.)
- Lateral development is governed by Molière Radius(R_M).

Properties of existing EMCals in HEP

	Materials	Granularity (mm^2)	Molière Radius (mm)
ALICE (PHOS)	$PbWO_4$	22 × 22	20
ALICE (EMCal)	Pb+Sc	60 × 60	32
ATLAS (FCal)	Pb+LAr	20 × 20	19
LHCb (ECal)	Pb+Sc	40 × 40	35
CMS (ECal)	$PbWO_4$	22 × 22	22
CALICE (Si ECal)	W+Si	10 × 10	~20
Future FoCal	W+Si	1 × 1	<15
FoCal prototype	W+Si	0.03 × 0.03	~10.5

Introduction

Physics motivation

Motivation

- Gluon density increases with Q^2 and $1/x$ (**Gluon Saturation**)
- Direct photons promise to be a very clean probe
- LHC provides opportunity to access small-x

$$x_{min} \approx \frac{2p_T e^{-y}}{\sqrt{s_{NN}}}$$

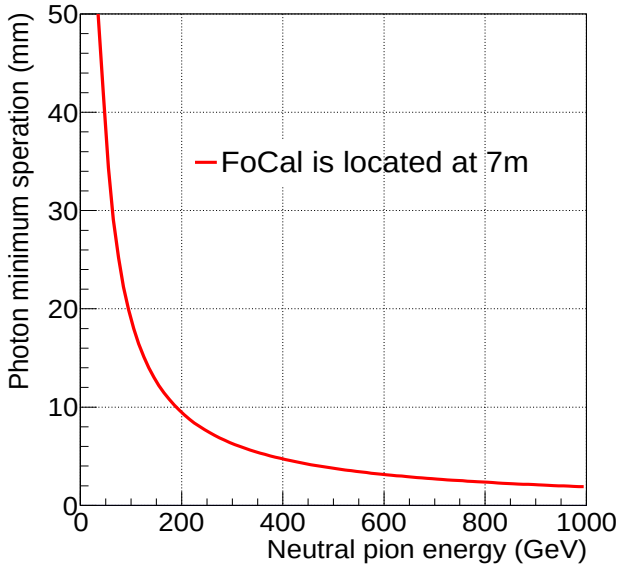

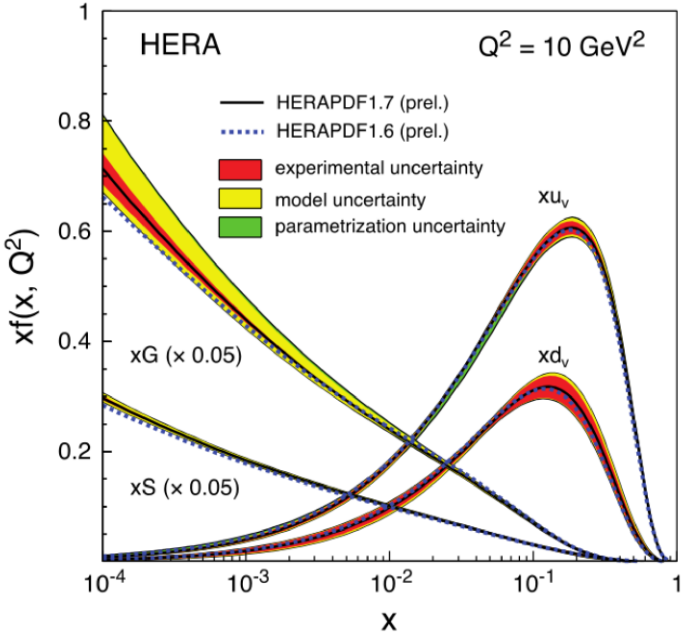

Probing small-x requires separation power in direct photon and decay photons from π^0

- High granularity detector
- Should allow 3D shower shape analysis and/or Particle Flow Algorithm

Introduction

FoCal upgrade proposal

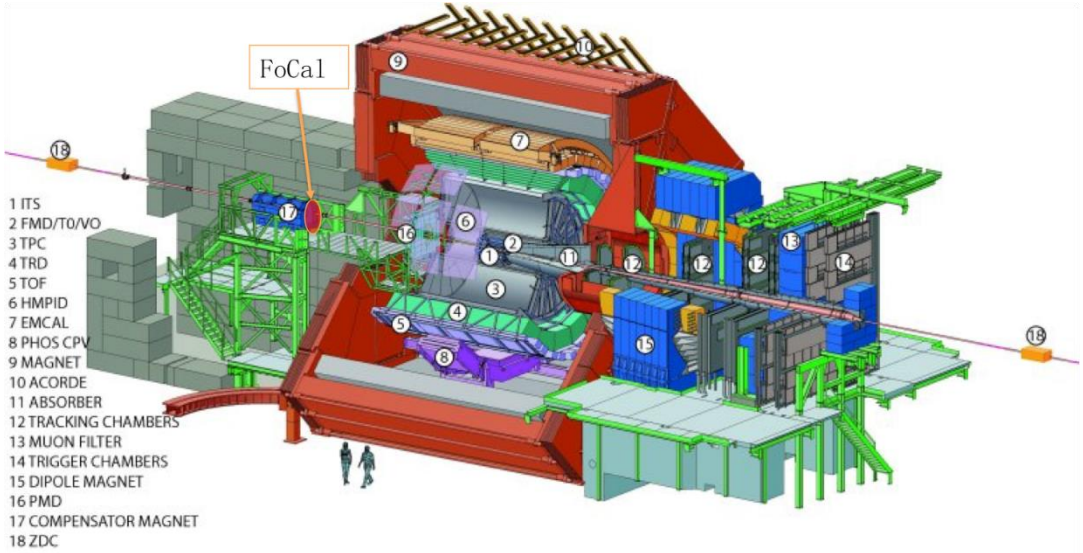

Proposed installation

- Proposal discussed in ALICE
- Outside the magnet of ALICE
- Focal-E + Focal-H
- Pseudorapidity : $3.5 < \eta < 5.3$
- ~7m away from interaction point

FoCal： TDR early 2020 -> Start production in 2022 -> Installation foreseen in 2024

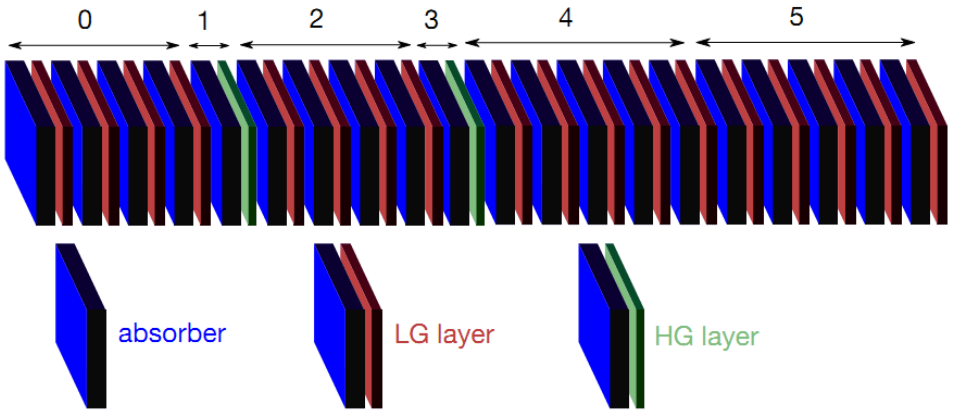

FoCal strawman design(FoCal-E)

- Hybrid layers
  - energy measurement+shower separation
  - LG : 1×1 cm^2, HG : 30×30μm^2
  - Pads + CMOS pixel sensors
- Analog + Digital readout
- Tungsten absorber (3.5mm ~ $1X_0$)

Design

The ALICE-FoCal MAPS Group


T. Peitzmann


G. J. Nooren


M. van Leeuwen


N. van der Kolk

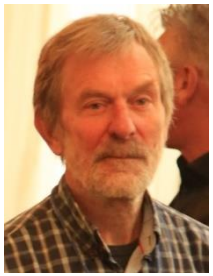
A. van de Brink


R. Barthel

- Part of CALICE collaboration.
- An international collaboration.
  Collaborating with Norway, Japan
- Clean room, mechanical, test.
- PhDs, masters and bachelors.


M. Reicher


C. Zhang

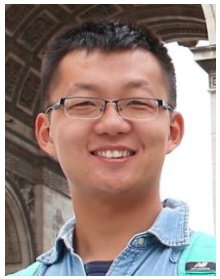
H. Wang

former PhDs

Design

MAPS sensor and its tuning

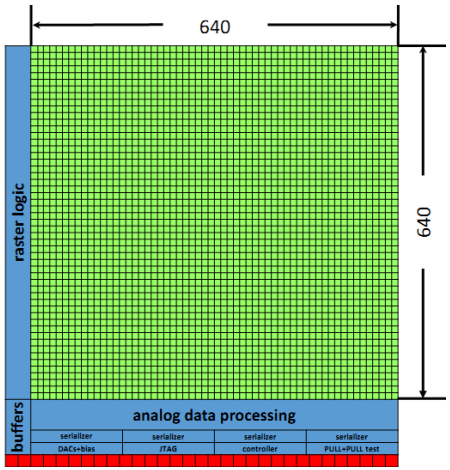

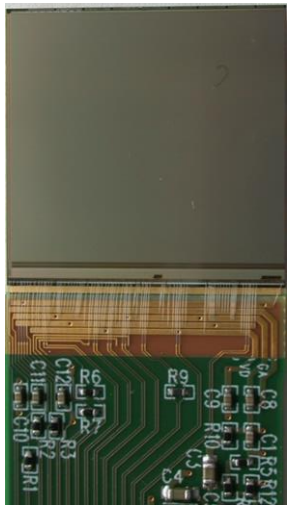

scheme of single sensor

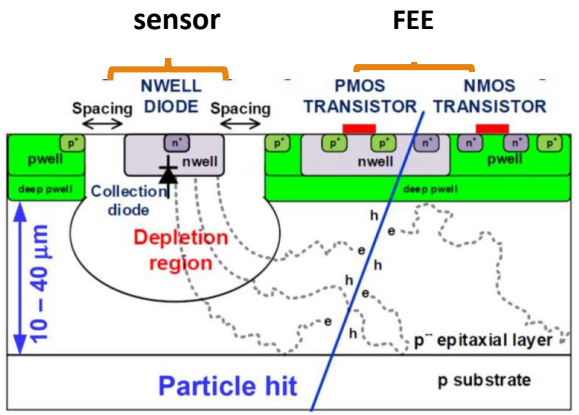

3 types of sensors in the prototype

thickness (μm)	resistivity ($\Omega \cdot$ cm)	number
15	400	46
20	400	31
14	10	19

- MIMOSA-23 PHASE-2
- 4 channels
- 640×640 pixels
- 1.92×1.92 cm^2
- 39M pixels in total (96 sensors)
- 642µs readout time

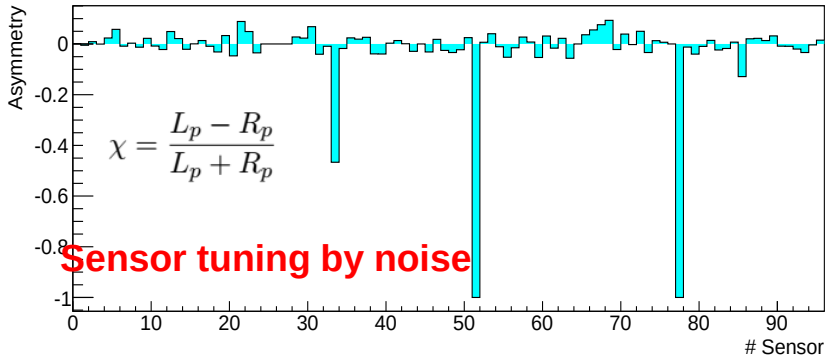

Design

Prototype

High granularity layers (HGL) need new technology, prototype built to perform generic R&D

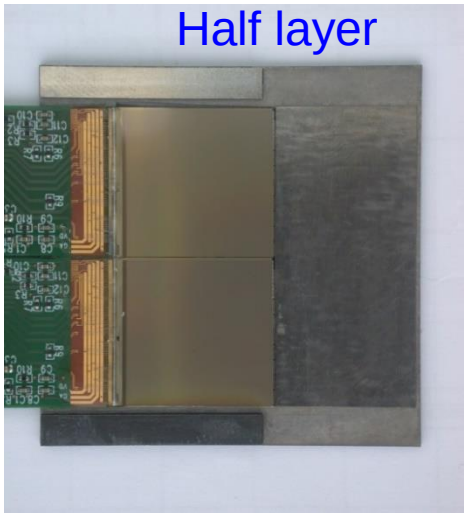

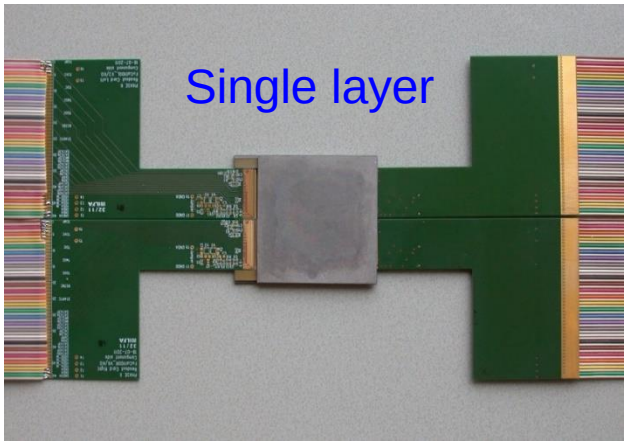

- 96 sensors
- 24 sampling layers
- W : absorber + cooling
- Water cooling of sensors
- 28 X_0 in total(0.974X_0/layer)
- 11mm Molière radius
- Overlap and gap region

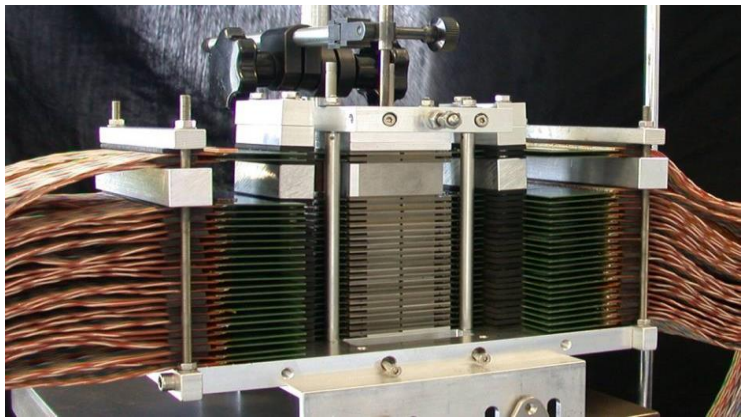

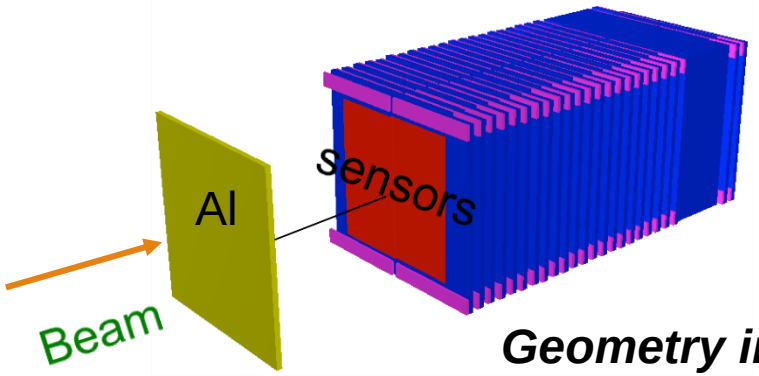

Geometry in Geant4

Design

Beam tests

Various energy and types of particles have been tested with this platform.

DESY 2014.02-2014.03

Germany

- e
- Energy : 2, 3, 4, 5.4 GeV

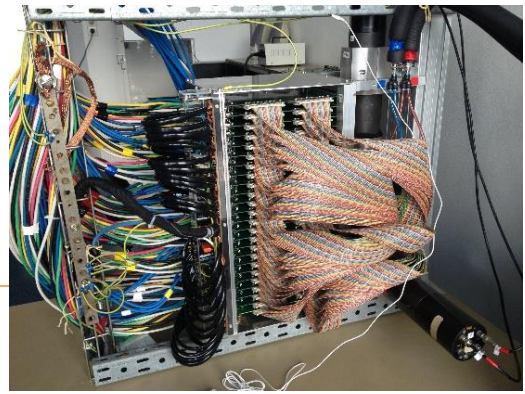

Utrecht 2014-2017

The Netherlands

- μ
- Energy : continuous

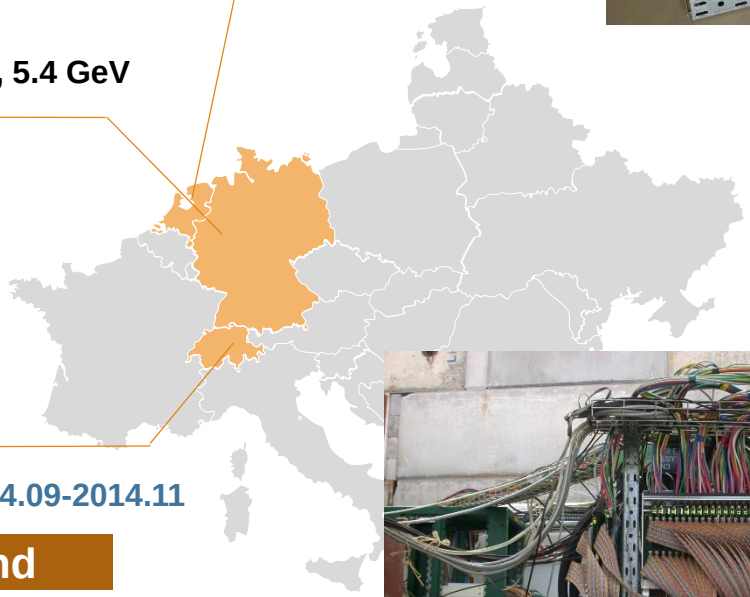

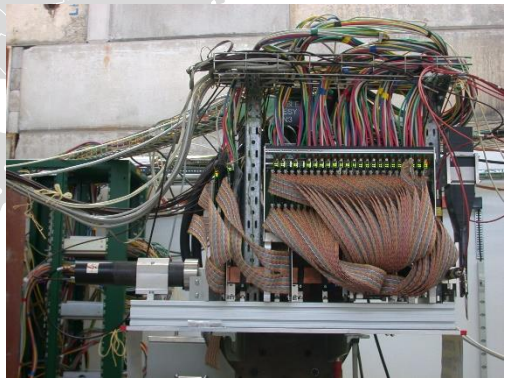

CERN 2014.09-2014.11

Switzerland

- e, π (Mixed)
- Energy : 30, 50, 100, 244 GeV

Measurement setup and data stream

Measurement Setup

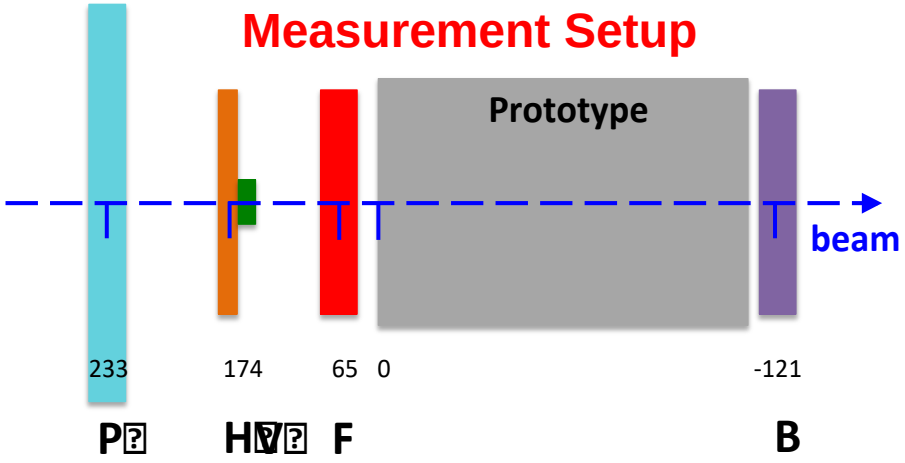

- Scintillators with different sizes.
- Different coincidence combinations of scintillators for beam and cosmic tests.

Data Stream Scheme

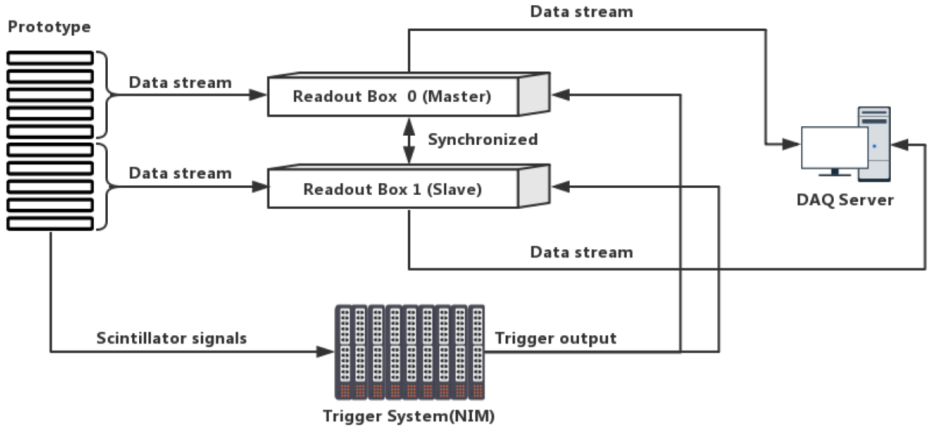

- Synchronization between 2 readout boxes.
- Data transmission by Ethernet cables.

  Sensors to boxes, boxes to DAQ
- 5 bits external NIM signals are sent to the boxes (scintillators).
- Sensors controlled by DAQ through slow control signals.

Design

Electronics

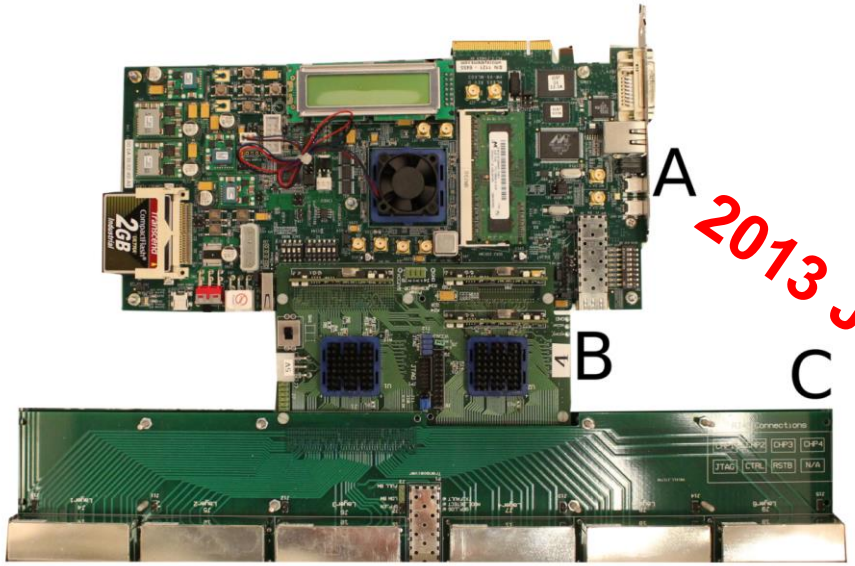

(A) Xilinx ML605 board
(B) Deserialization board
(C) 2 fan out board

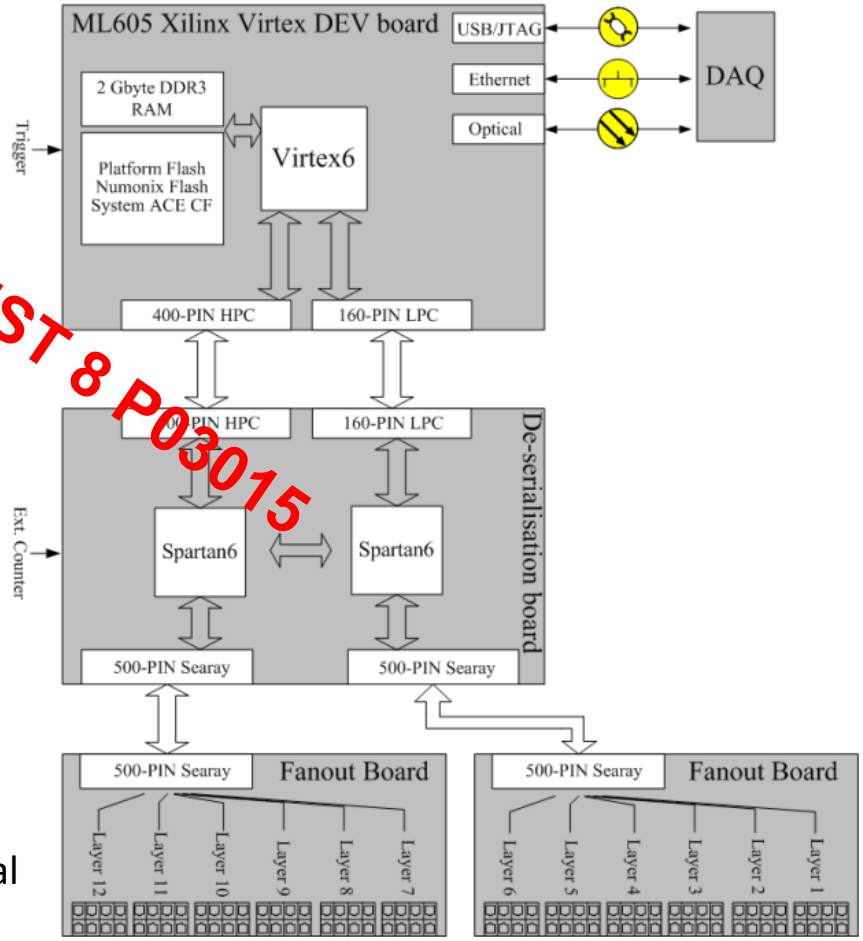

- Data acquisition is driven by internal/external trigger signal.(for different beam modes)
- Data bits and internal counter for recording external triggers.

Raw Data Quality (Challenges)

Data Quality

Map of hits distribution

Raw Data

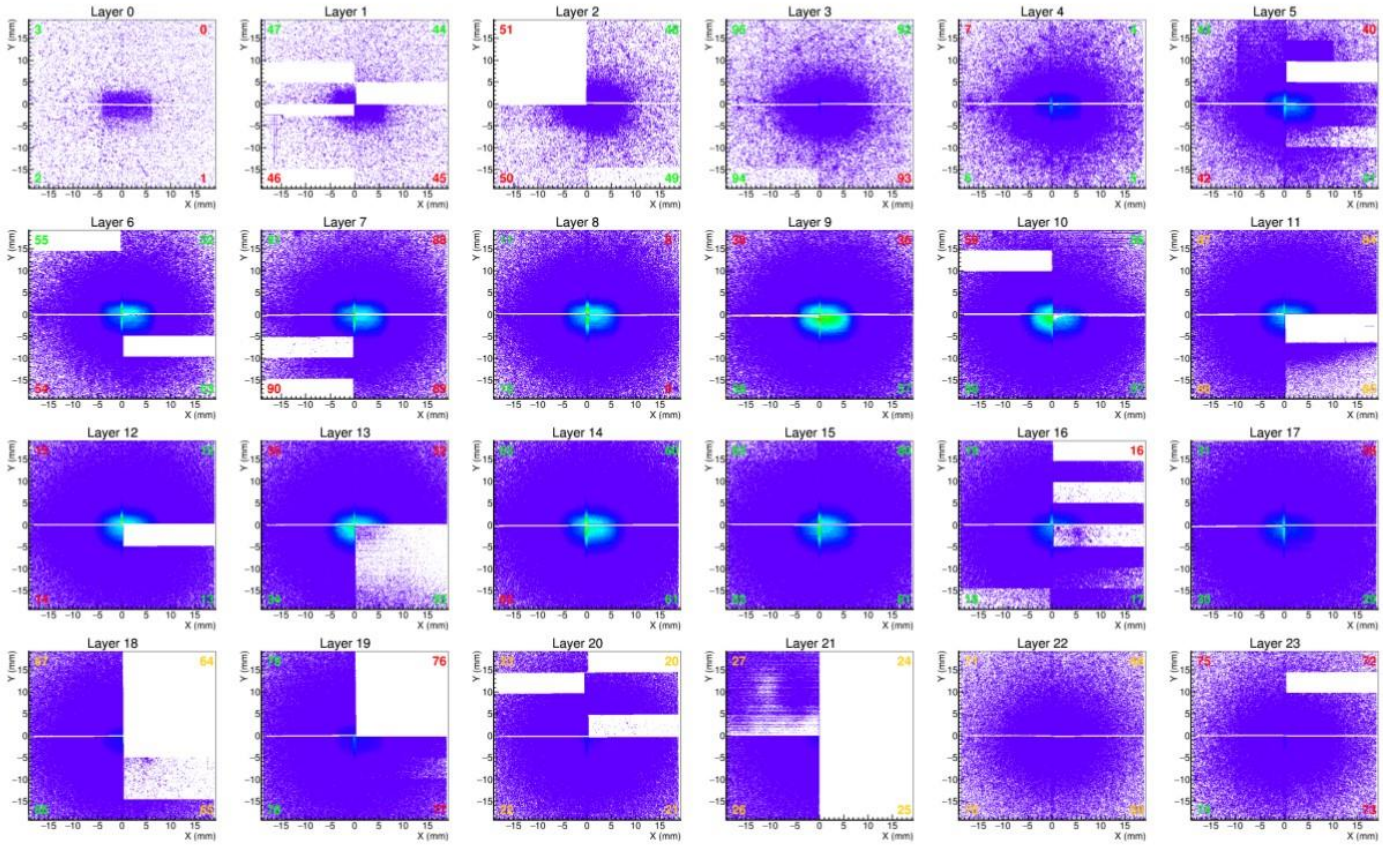

Challenges !!

- Dead sensors.
- Dead channels.
- Hot lines/columns.
- Unstable/Malfunctioning sensors/channels.
- Sensitivity imbalance.

Data clean is required.

- Ban dead sensors.
- Remove bad runs, bad spills.
- Remove problematic channels.
- Remove hot pixels.
- Steering balance.

Data Quality

Cluster size

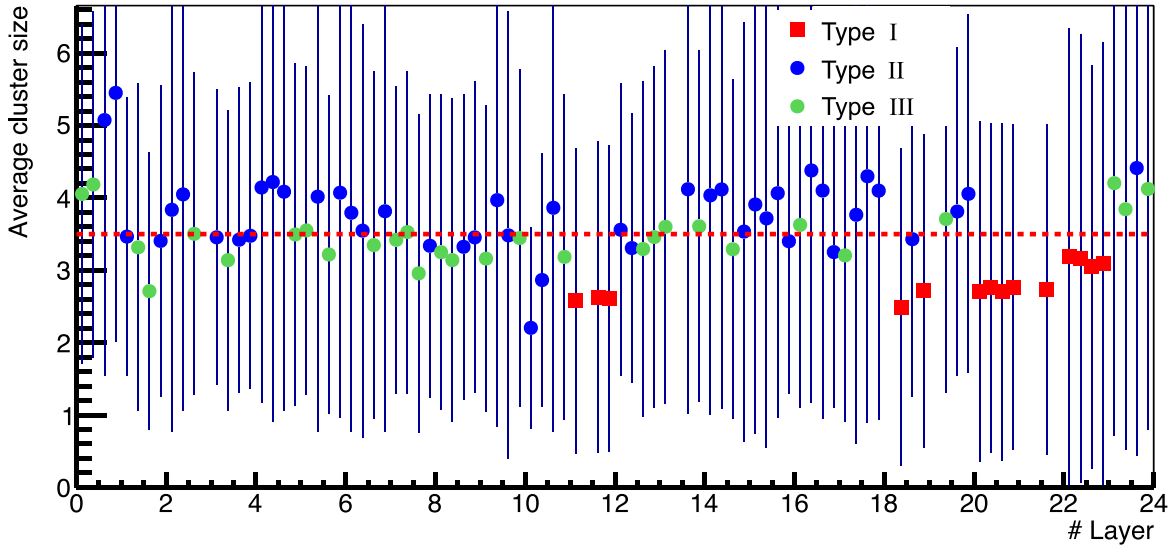

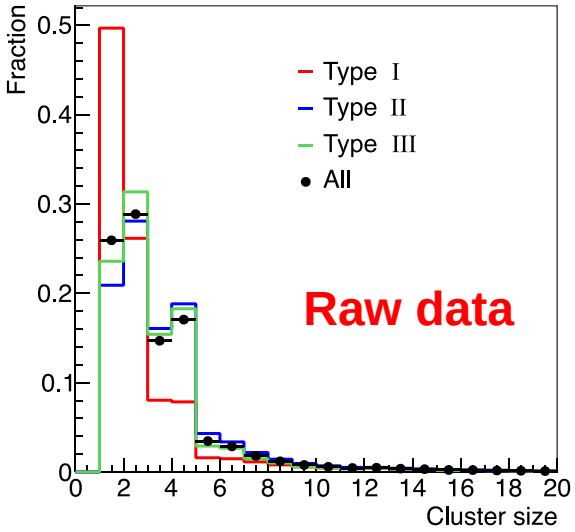

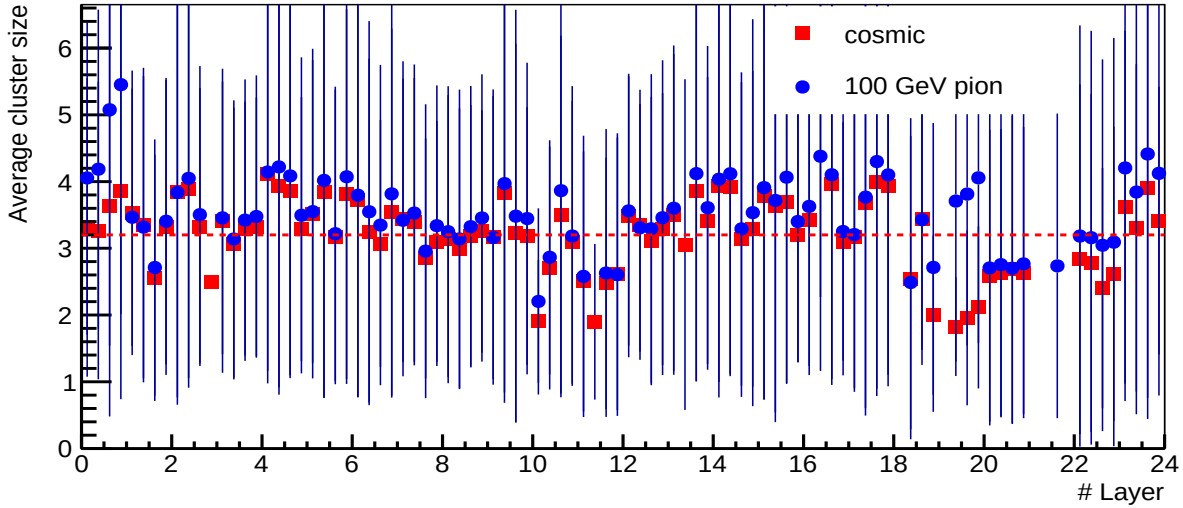

A significant difference of average response for tracks are observed.

Calibration is necessary !!

Data Quality

Raw longitudinal profiles

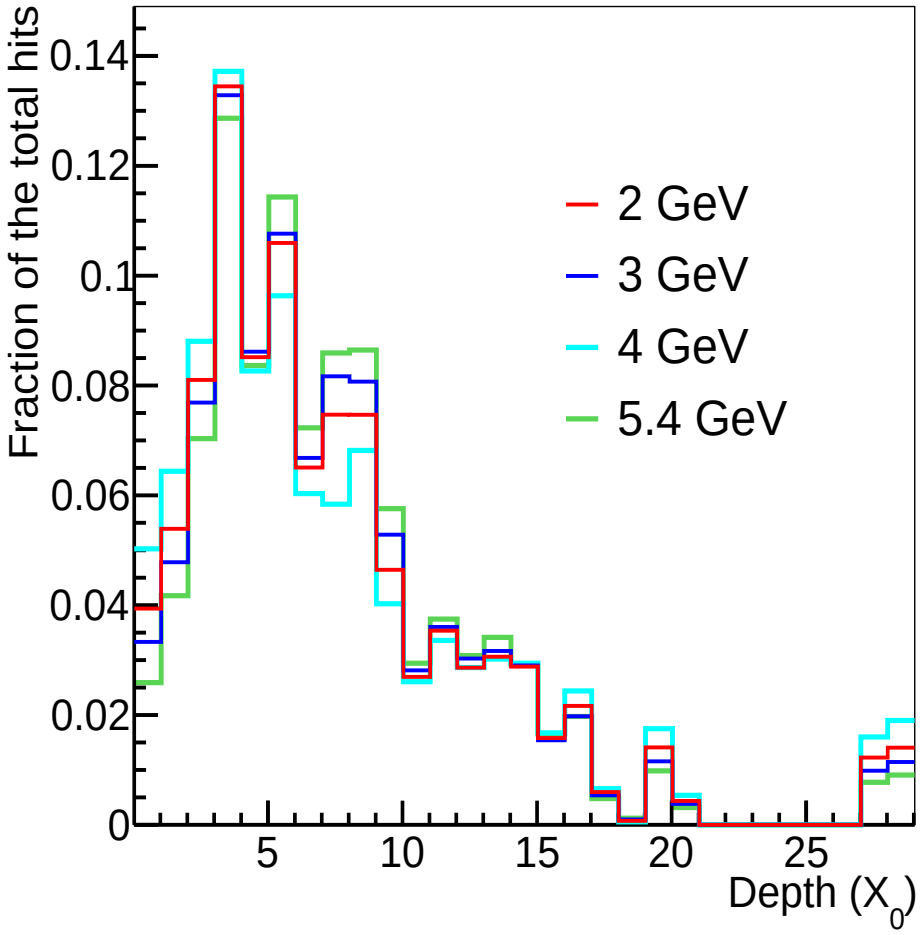

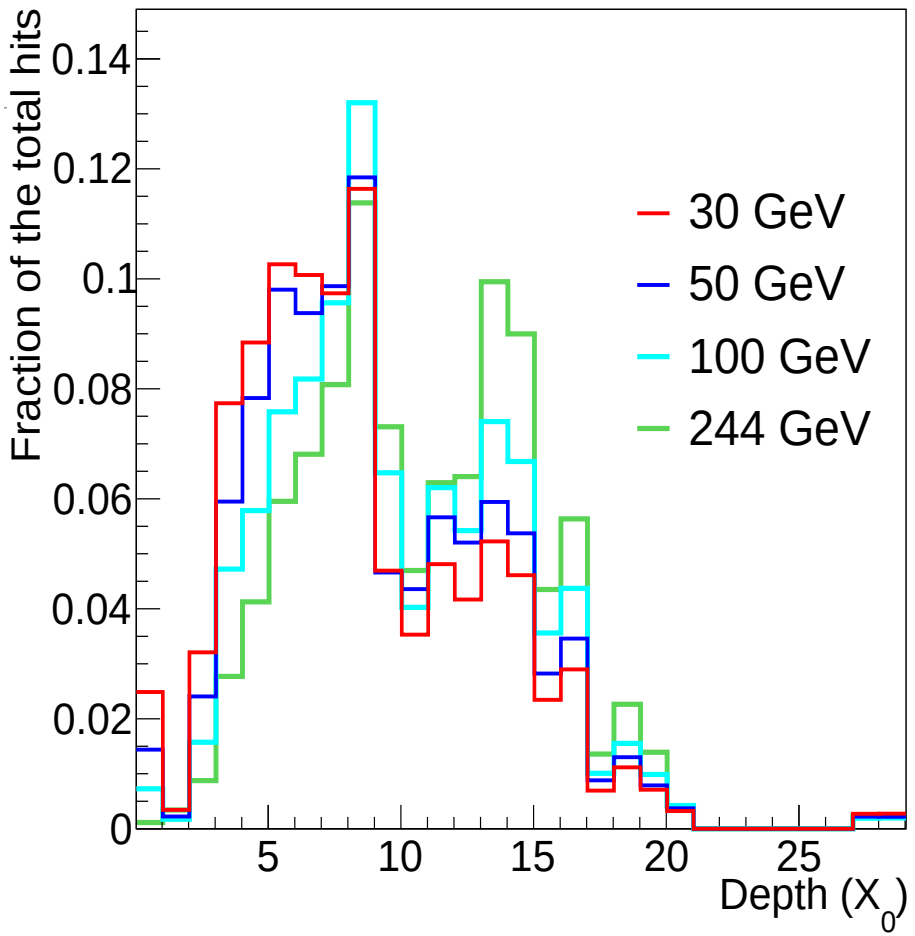

Irregular responses between layers.

Calibration is necessary !!

Test Beam Data Analysis

Test Beam Data Analysis

Event selection

Width VS Number of hits : To select electron candidates.

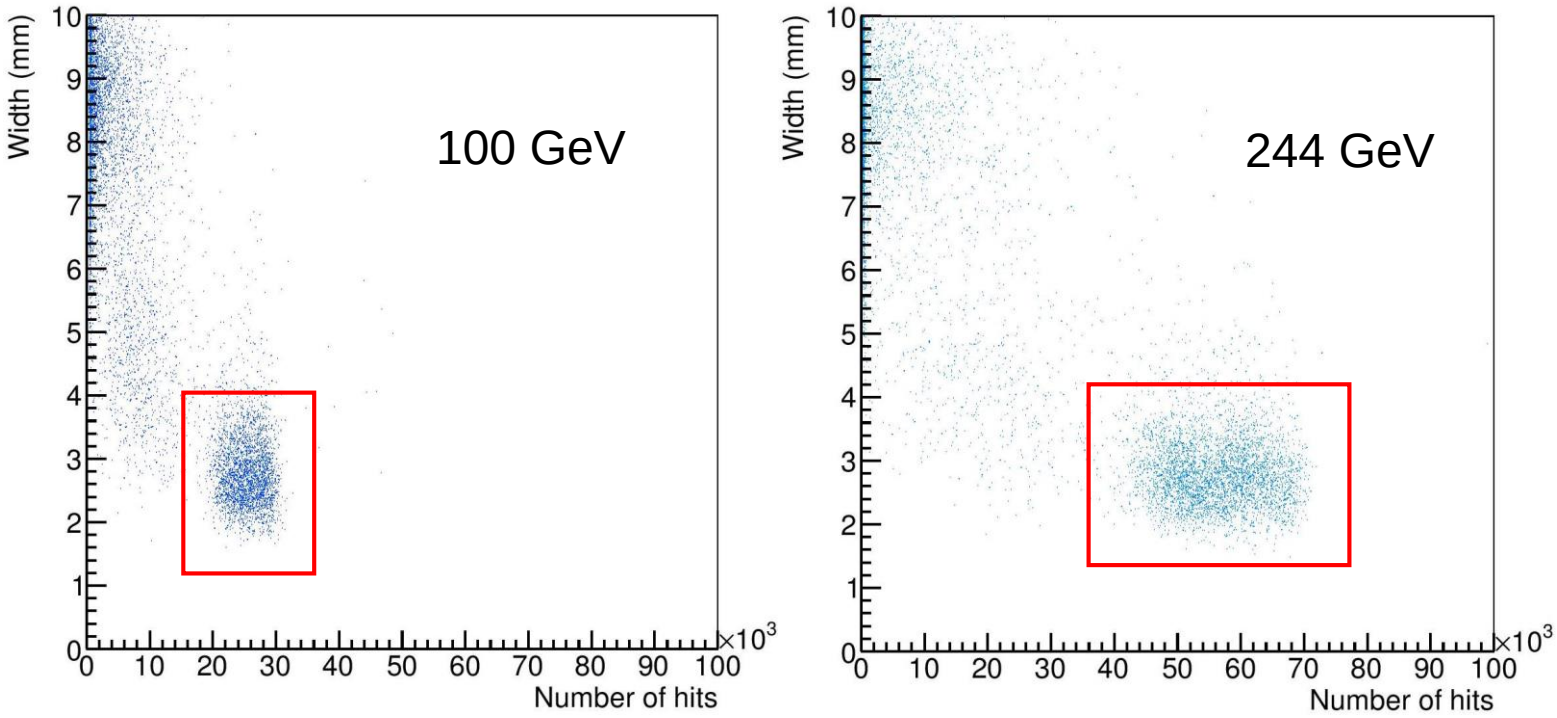

Width: The distribution of the standard deviation of hit positions in layers 3 and 4 (layers with sensors all working).

Test Beam Data Analysis

Contamination estimation

TempleteFit to estimate the fraction of pion contamination

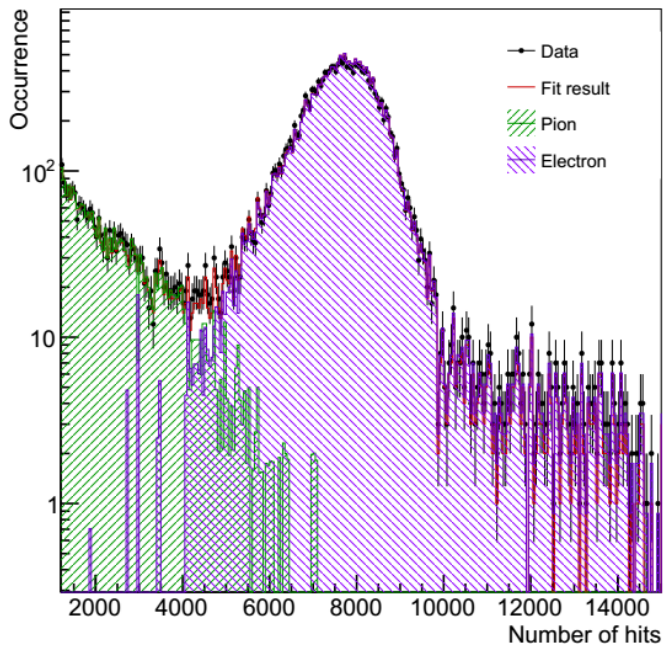

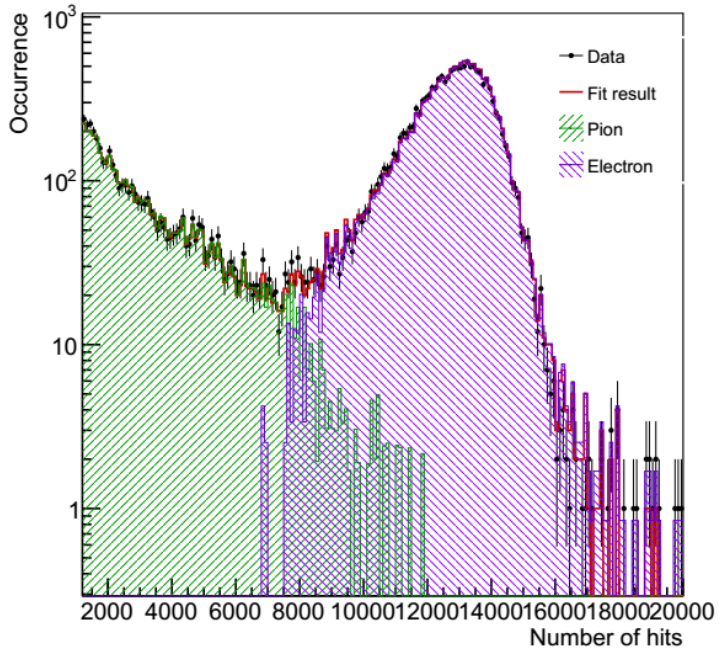

energy(GeV)	fit range	hits cut	pion left	contamination(%)
30	150-70000	5800	24	0.2
50	300-70000	9500	39	0.3
100	1200-70000	18000	216	1.0
244	900-70000	40000	55	0.9

With proper cut on number of hits, the hadron contamination can be ignored.

Test Beam Data Analysis

Position correction

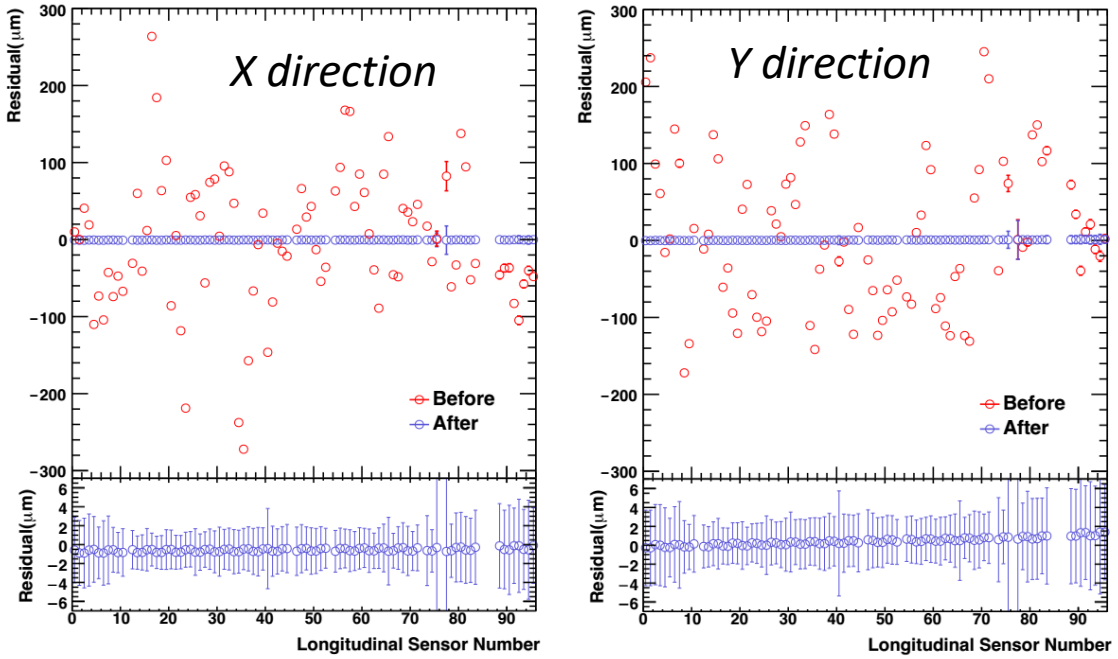

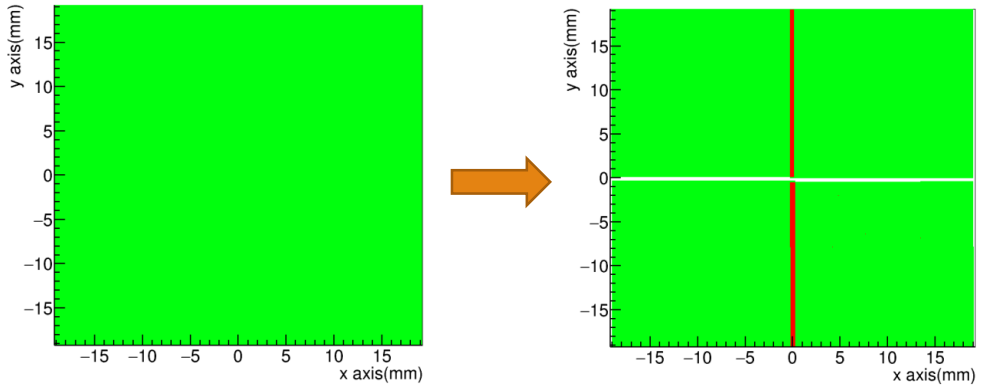

Objective: to reconstruct the real position of the pixels.

$$X_{new} = X_{old}\cos\theta + Y_{old}\sin\theta + \Delta X,$$
$$Y_{new} = Y_{old}\cos\theta - X_{old}\sin\theta + \Delta Y$$

- 3 DOFs for every sensor.
- In total 283 DOFs in alignment.
- Use cosmic muons, with iterative method.
- Cross check with pion data.
- Fix two sensors to remove "weak mode" effects.

Test Beam Data Analysis

Inclination Correction

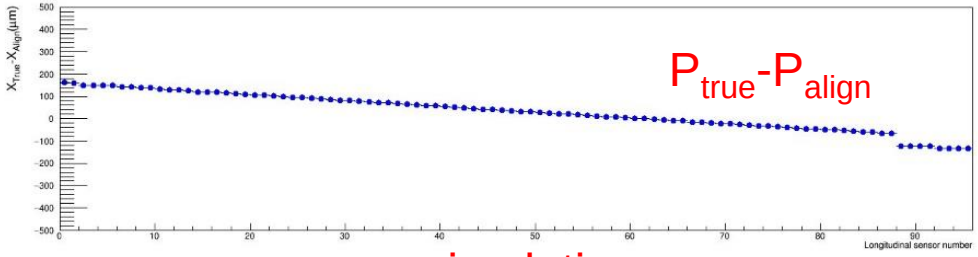

simulation

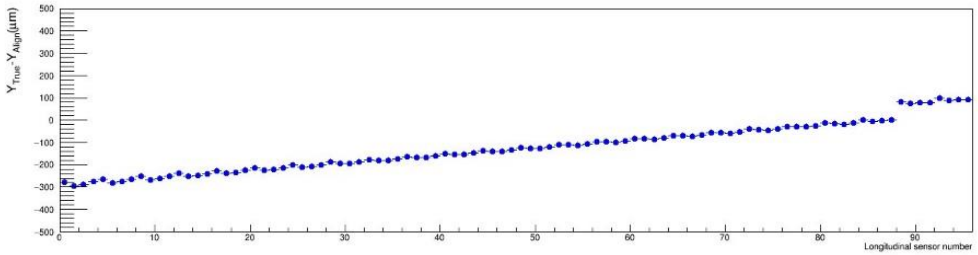

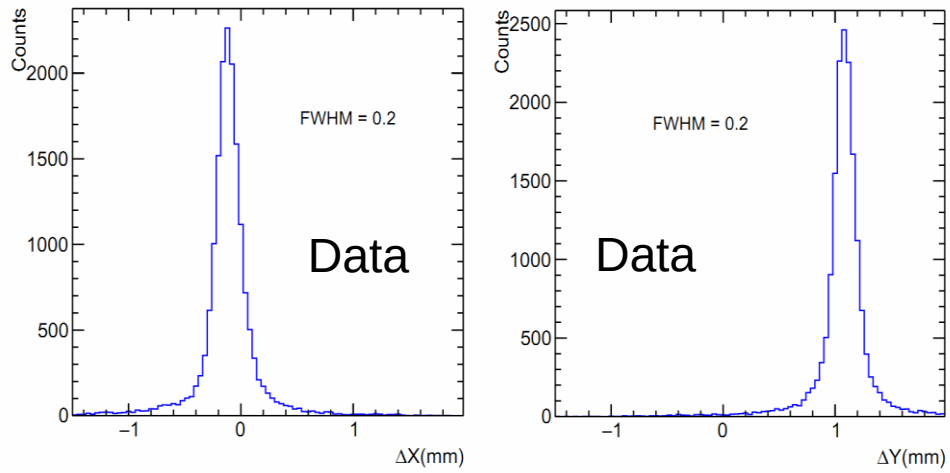

Apparent transverse shift of sensors with linear dependence on longitudinal position: most likely explained by relative inclination of the beam direction.

- Related to weakly defined DoF from alignment(no constrain on orientation of z direction).

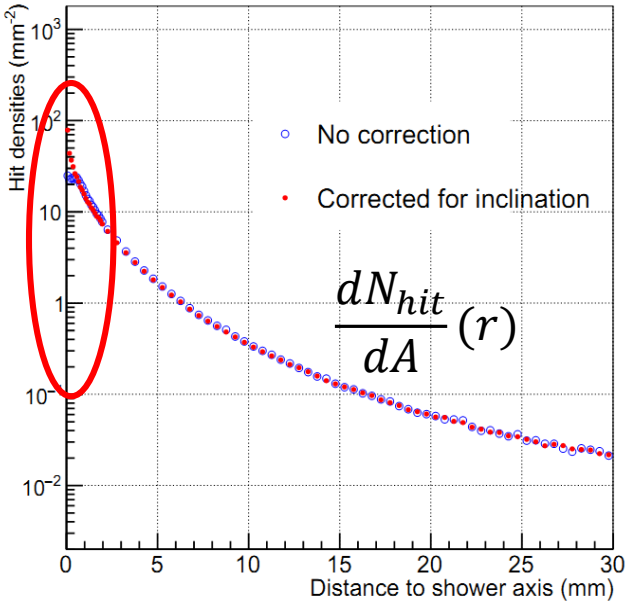

Test Beam Data Analysis

Shower position

Objective: crucial for shower profile analysis and two-shower separation.

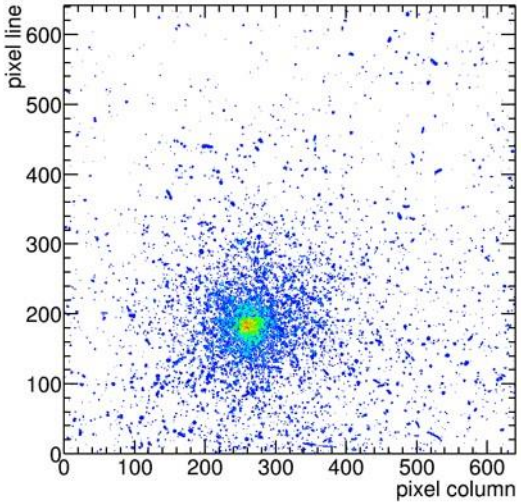

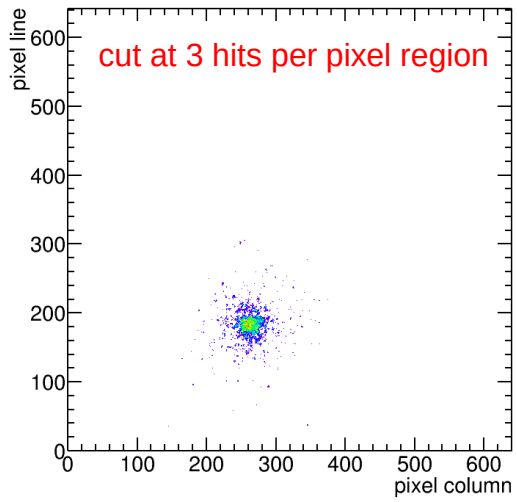

$$X_c = \frac{\sum_i w_i^n x_i}{\sum_i w_i^n}$$

$$w_i = \sum_L R_{l,i}$$

$$(R_{l,i} = 0 \; or \; 1)$$

Method

- Use information of all good layers to reconstruct the shower center.
- Refine the shower core region by setting cut on amplitude in pixel region.
- Use power law weight to make shower core region more significant.

Test Beam Data Analysis **Correction for dead area**

No signal available from part of the sensors (dead, noisy, …):
compensation for dead area (16.7% of total pixels)

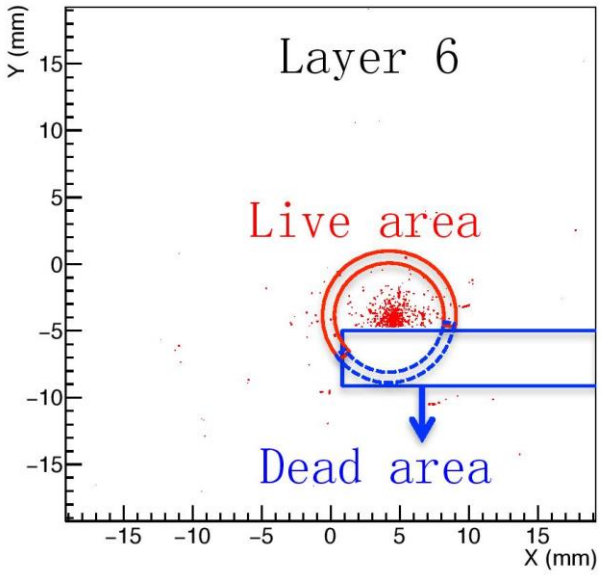

Case 1: $N_{pixels} > 0$

Hit density obtained from the live pixels in the ring.

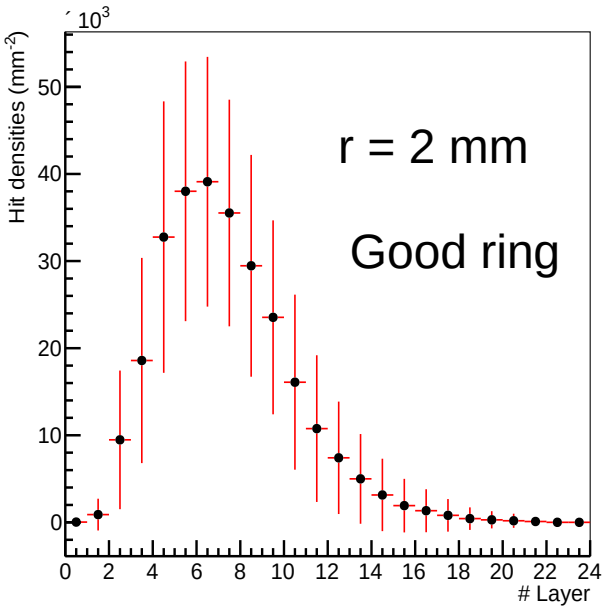

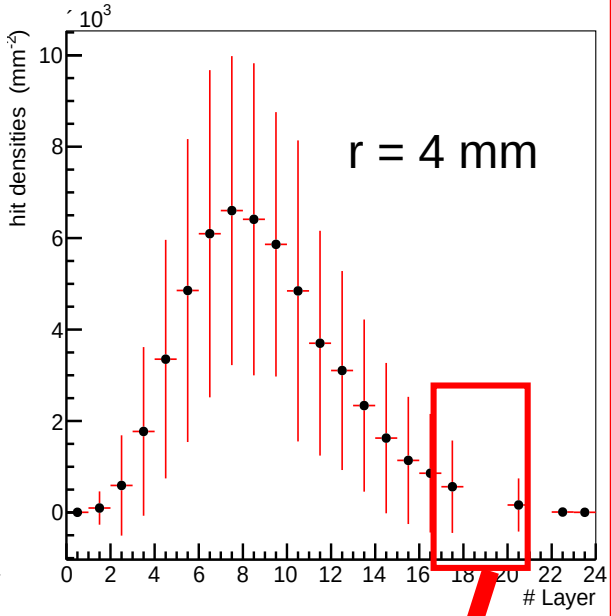

Case 2: $N_{pixels} = 0$

$$\rho_l(r) = \rho_{l-m}(r) + m/(m+n)\,[\rho_{l+n}(r) - \rho_{l-m}(r)]$$

The hit density obtained from neighboring good layers

Test Beam Data Analysis

Relative sensitivity calibration within a layer

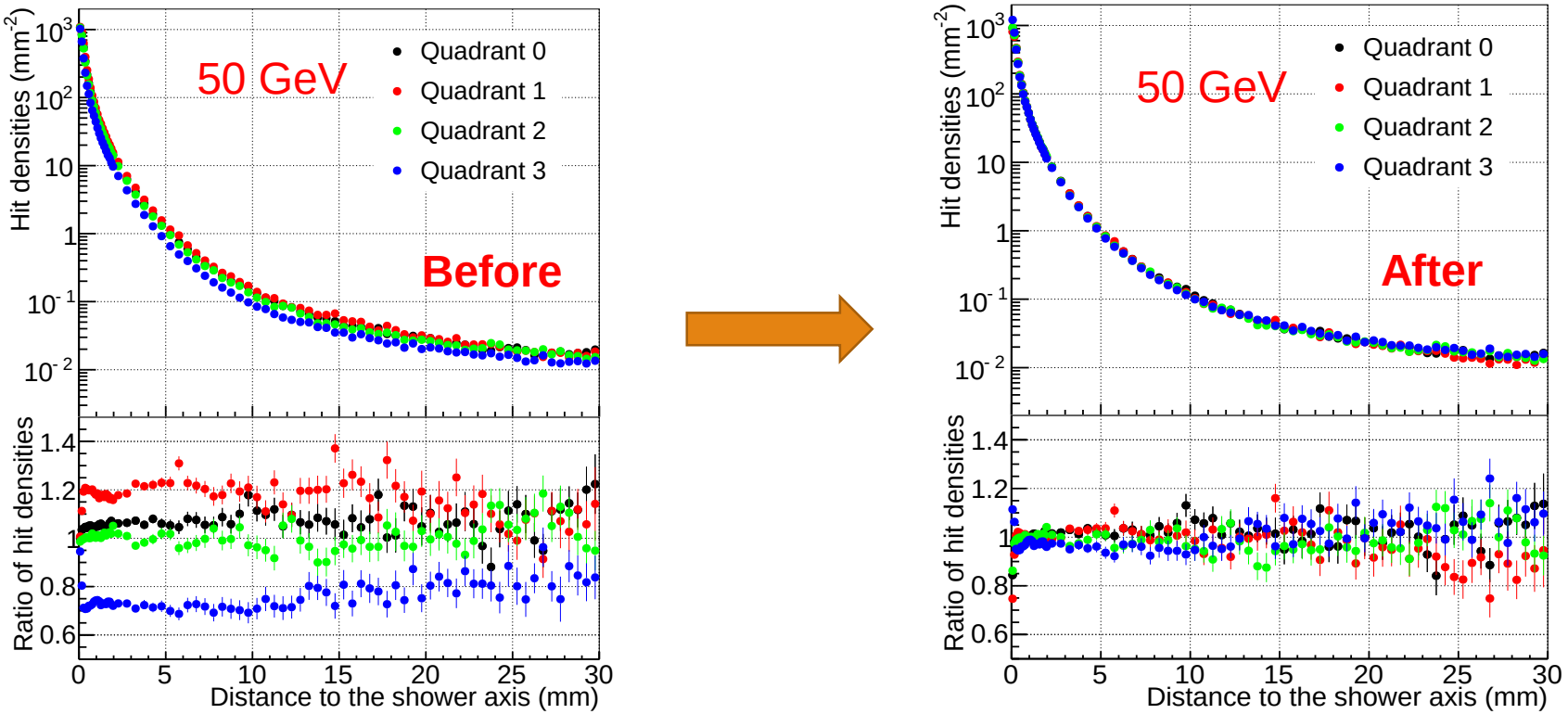

- The sensitivity varies from sensor to sensor before calibration in a layer.
- These instrumental effects can affect the detector performance(energy resolution).

Test Beam Data Analysis

Response calibration between the layers

- calculate hit density in rings around shower center
- equalize response of the 4 sensors in each layer
- relative layer-to-layer calibration with gamma distribution

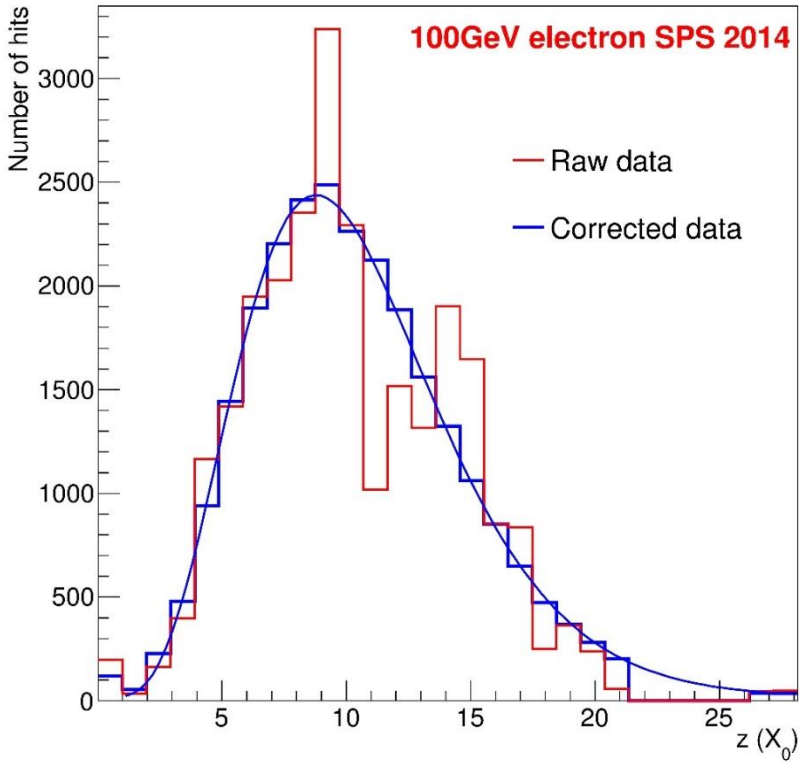

$$N(t) = N_0 b \frac{(bt)^{a-1} e^{-bt}}{\Gamma(a)} (t = x/X_0)$$

- Blue curve is fit curve to the blue histogram which indicates the longitudinal profiles obtained from the selected good sensors (one sensor per layer).

Simulation

Simulation

Charge diffusion & noise model

$$\rho(\vec{R}) = \rho(r,\phi) = \frac{d\Omega}{4\pi}\cdot\exp\left(-\frac{|R|}{\lambda}\right) = \frac{1}{4\pi L(h^2+r^2)^{\frac{3}{2}}}\cdot\exp\left(-\frac{\sqrt{h^2+r^2}}{\lambda}\right)drd\phi$$

- Isotropic diffusion & attenuation.
- Two parameters to control the model.
- keep the average cluster size is same.

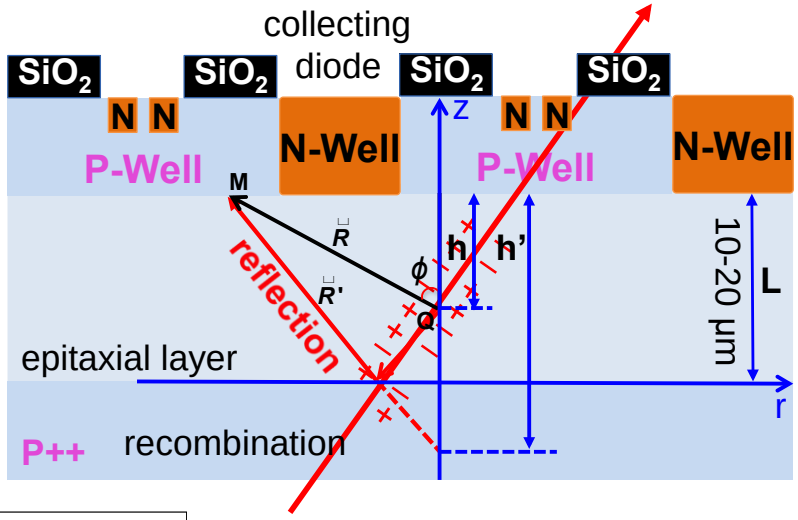

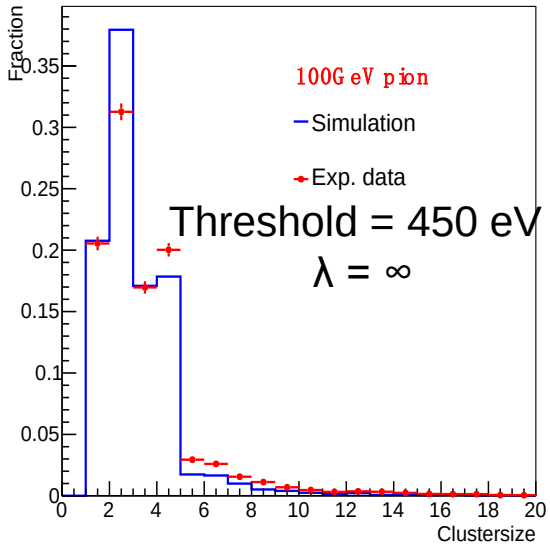

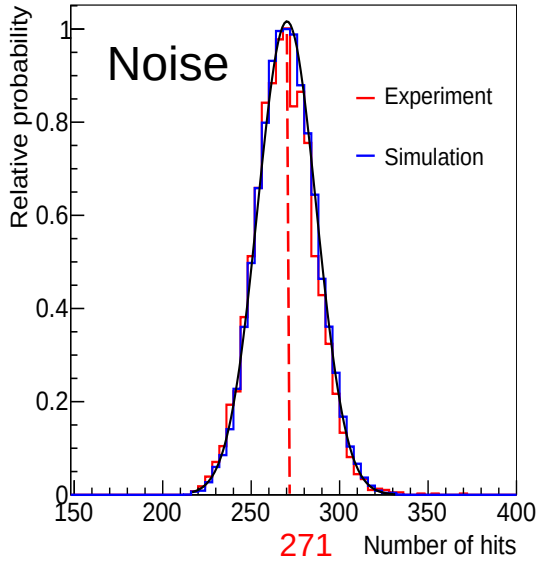

1. Generate the number of noise hits in each sensor:

$$N_{noise} = Possion(\overline{N_{noise}})$$

2. $\bar{N}_{noise}$ is obtained from exp data

Simulation

Limitation of interpolation for dead areas

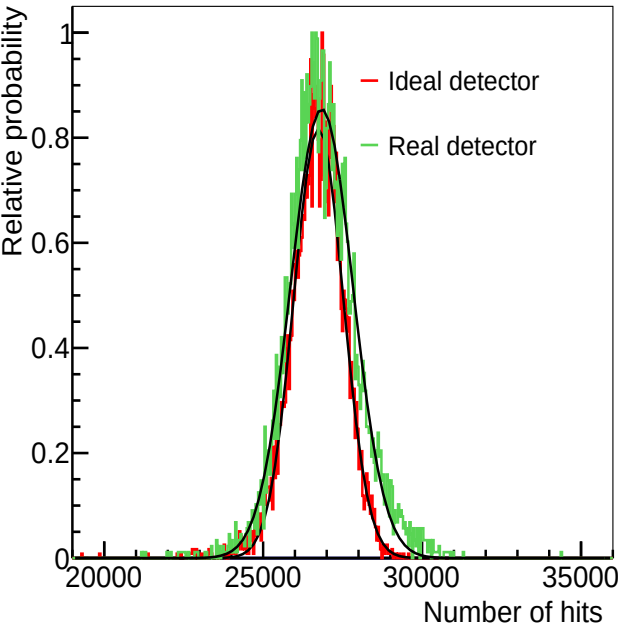

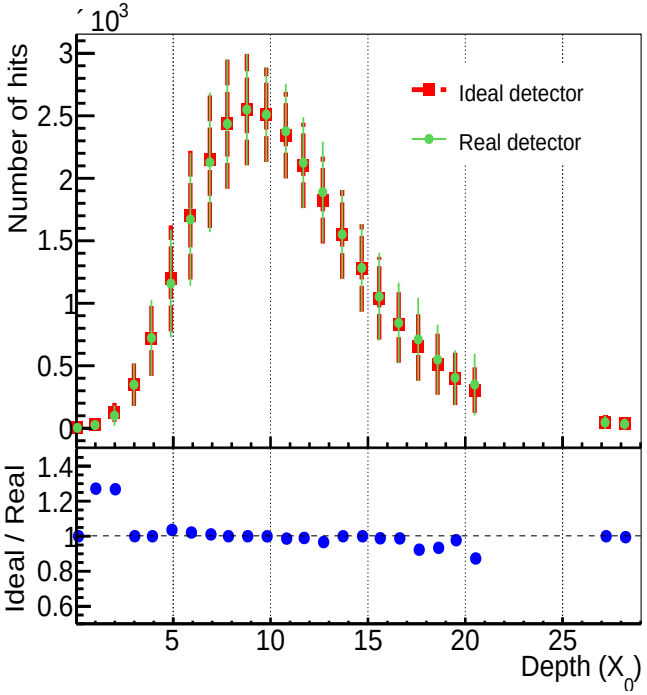

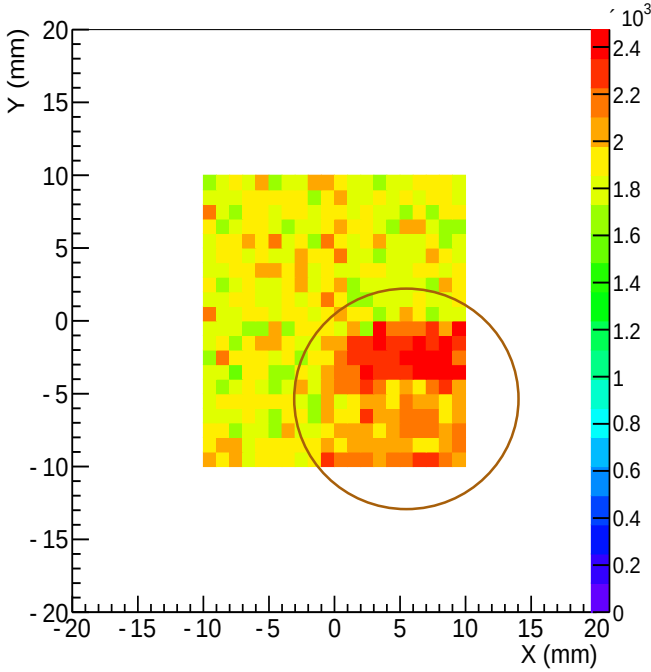

Limitation of interpolation for dead areas are studied by comparison with ideal detector.

- wider hits distribution.
- leads to a bias of number of hits and larger fluctuations.
- not fully estimate the number of hit in dead area.

Results

Results

Linearity

Scenario	k (GeV^{-1})
Data	266.9 ± 0.01
MC (real detector)	262.6 ± 0.2
MC (ideal detector)	258.2 ± 0.01

Scenario	α (GeV^{-1})	β
Data	292.2 ± 0.6	0.980 ± 0.0004
MC (real detector)	277.0 ± 0.8	0.988 ± 0.0006
MC (ideal detector)	278.7 ± 0.7	0.986 ± 0.0005

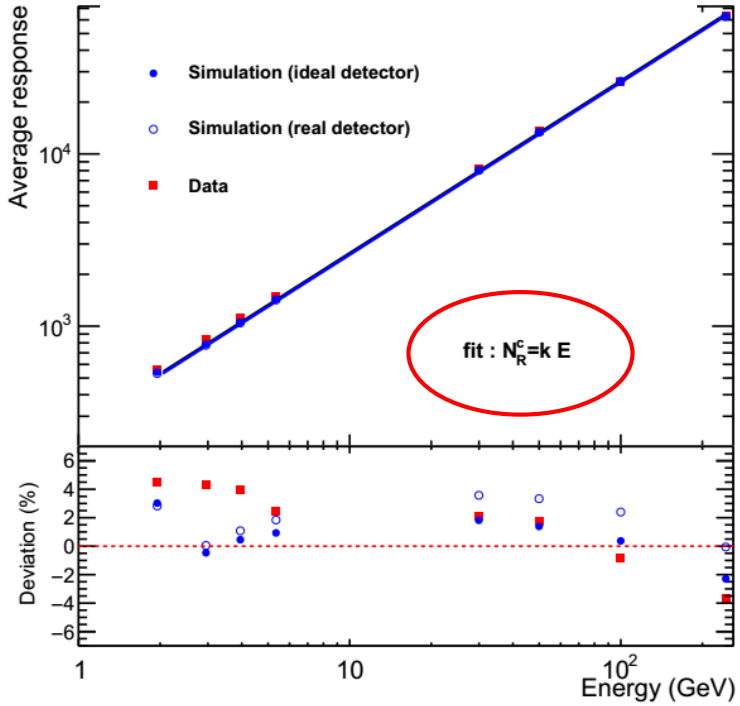

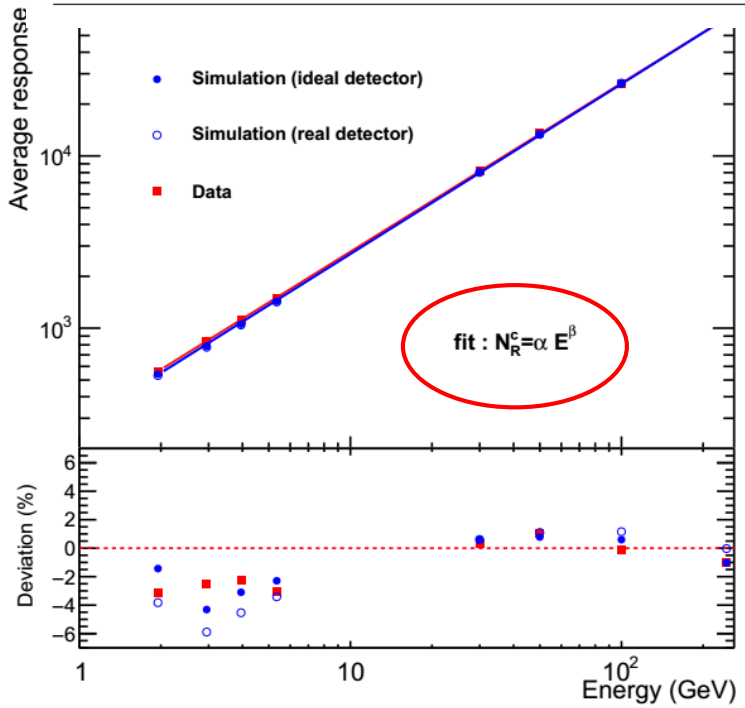

- Comparison of linear and power law fit of mean response of the detector for different energies.
- Left: The data shows an decreasing deviation to higher energies. (saturation??)
- Right: Discrepancy points to an uncertainty in the relative calibration of the two different measurements.

Results

Energy & position resolution

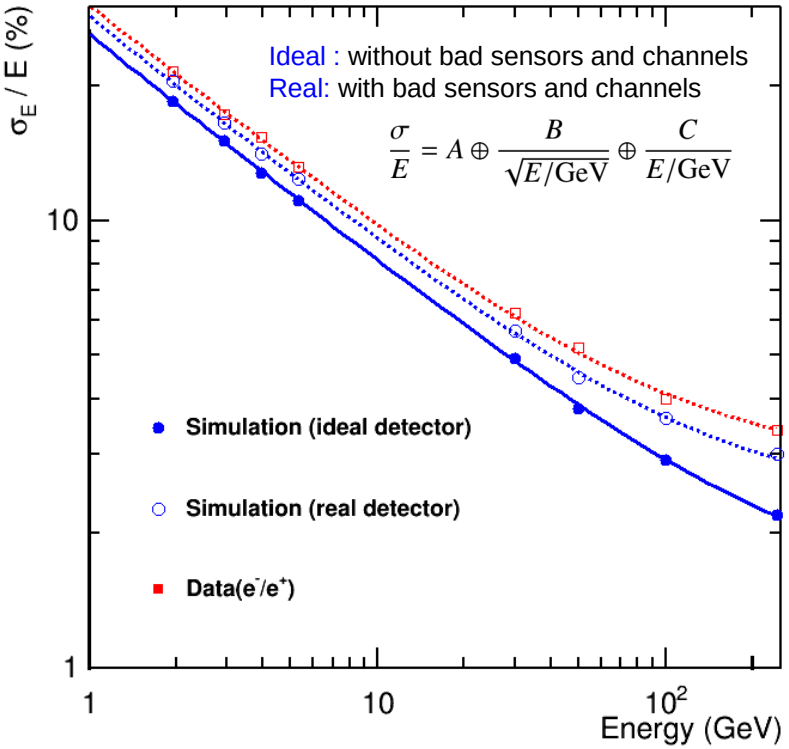

Calibration	A(%)	B(%)	C(%)
optimized	2.95 ± 1.65	28.47 ± 3.83	6.3

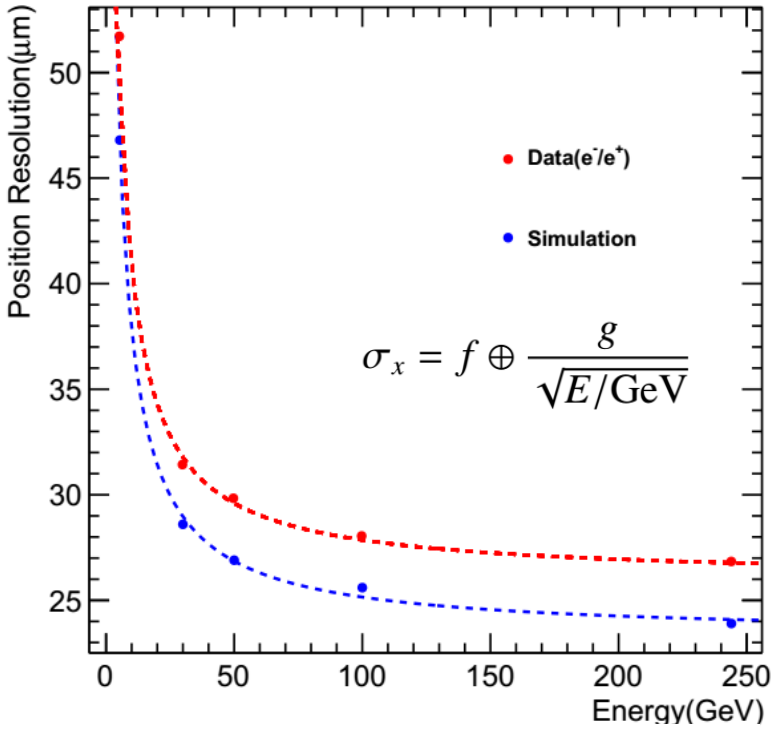

Data source	g (μm)	f (μm)
experimental	103.76 ± 1.16	25.80 ± 0.25
simulation	94.11 ± 1.05	23.33 ± 0.22

- Sensitivities of sensors are not fully equalized.
- Energy spread of beam is not implement in MC.

- Good agreement between EXP and MC.
- Slight difference may due to alignment.

Results

Lateral hit density profiles

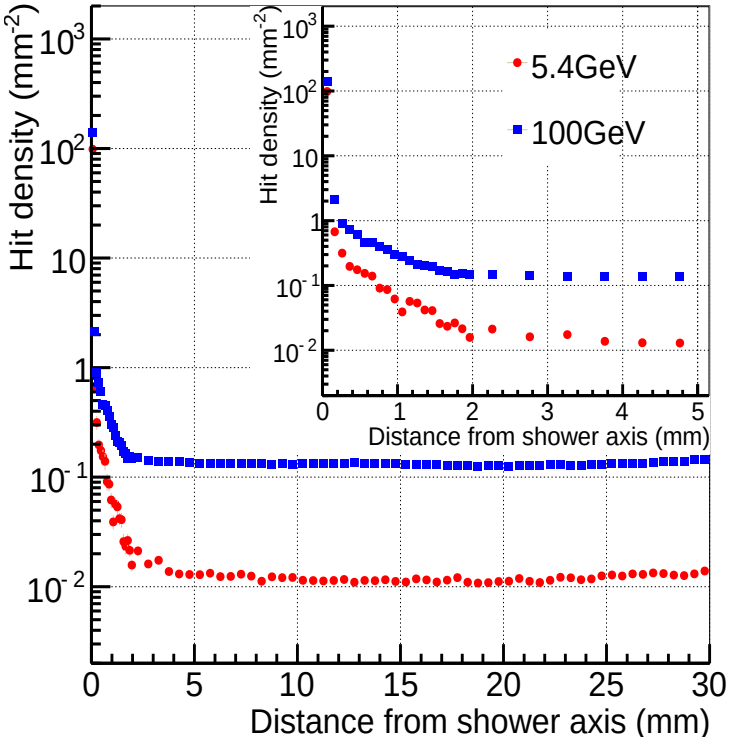

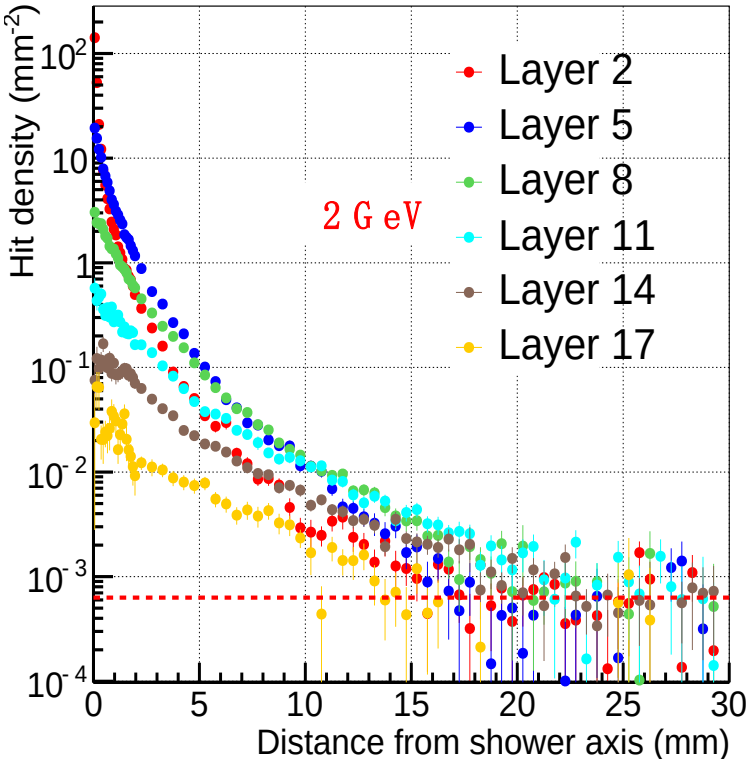

- Clear difference of noise rate due to threshold setting.
- Sharp peak corresponds to ~3 hits/event, similar to MIPs.
- Standard deviation of peak is ~0.04 mm, accurate shower center determination.
- Tail due to early conversions and back scattering.(similar to MC)

Red dash line indicates the noise fluctuations.

Lateral hit density profiles

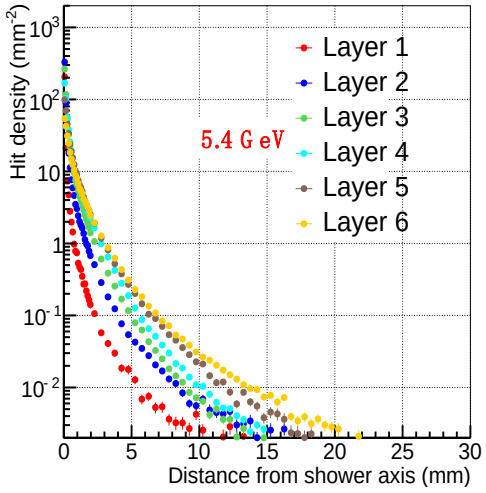

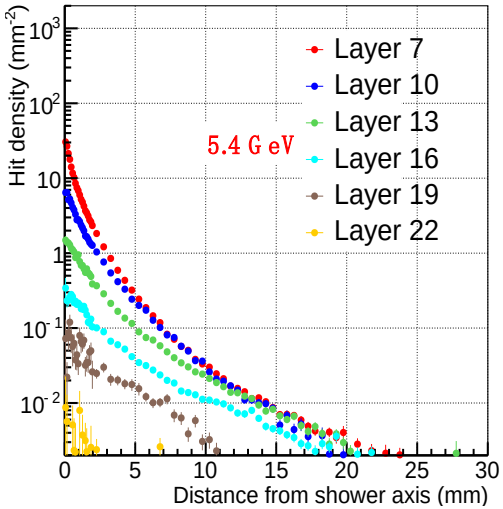

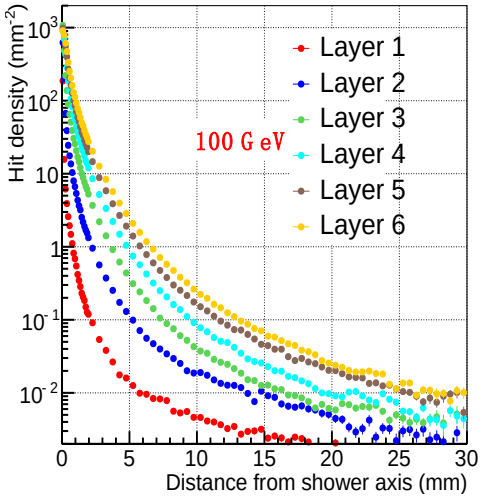

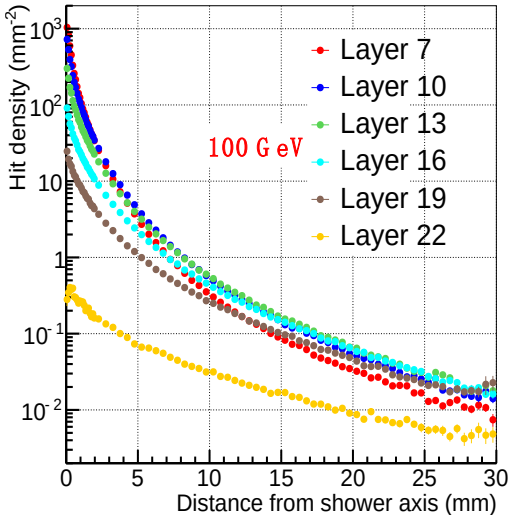

- The steepness of the hit densities decrease with increasing shower depth.

- Unprecedented detail of shower development (layer by layer).
- Potential parameterization of the shower profile.

Distribution of hit density

Distribution of hit density in longitudinal direction at selected *r*

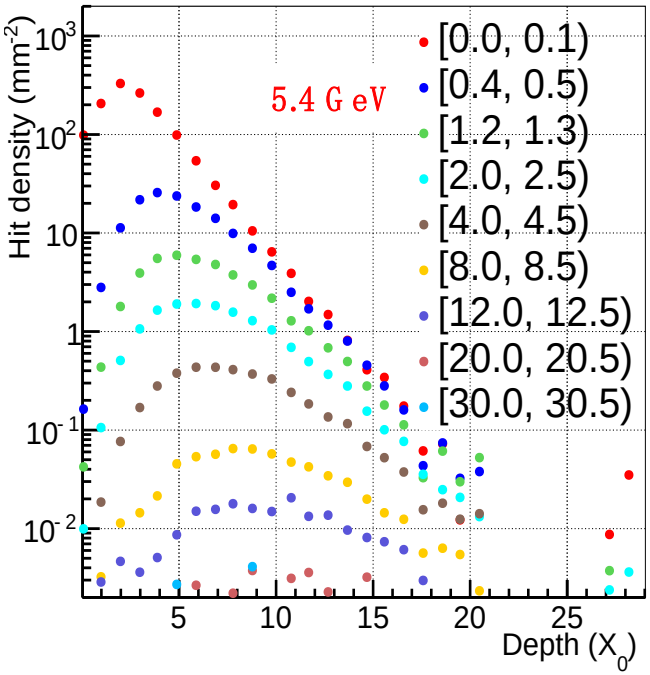

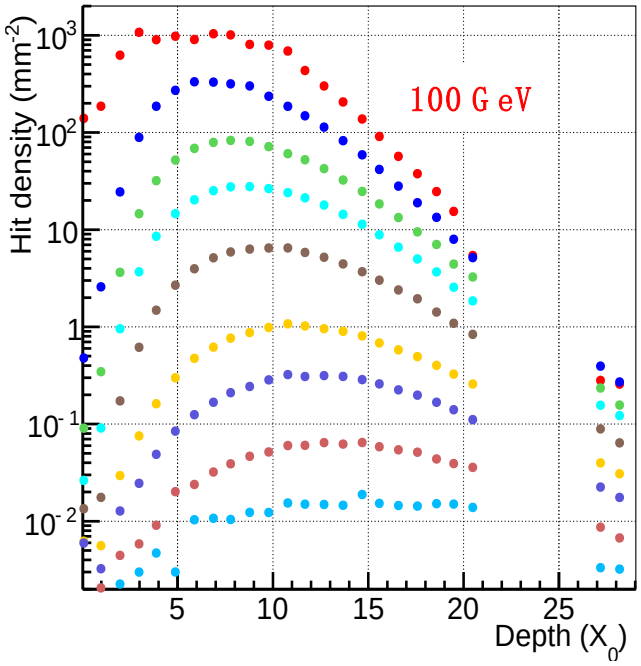

- The maximum hit density moves deeper with increasing r.
- For higher energy, the pattern changes slower than for lower energy.

Results

The quality of fitting lateral profile with functions.

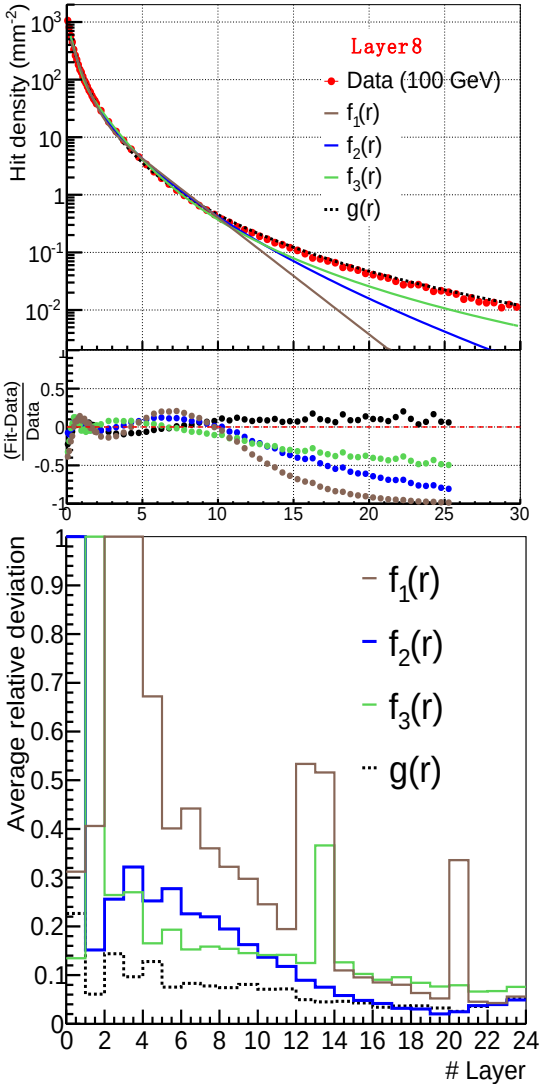

$$f_1(r) = A1[p \cdot \exp(-r/\lambda_1) + (1-p) \cdot \exp(-r/\lambda_2)]$$

$$f_2(r) = A1[p \cdot \exp(-\sqrt{r/\lambda_1}) + (1-p) \cdot \exp(-r/\lambda_2)]$$

$$f_3(r) = A1[p \cdot \frac{2R_1^2}{(r^2+R_1^2)^2} + (1-p) \cdot \frac{2R_2^2}{(r^2+R_2^2)^2}]$$

$$g(r) = p0(1+\frac{r}{p1 \cdot p2})^{-p1}$$ **Best !**

$$\sigma_l = \sqrt{\frac{\sum_{i=1}^{N} d_l^i(r)^2}{N}}, d_l^i = \frac{\rho_{fit}(r) - \rho_l(r)}{\rho_l(r)}$$

We conclude that the best fit function is g(r), and the fit quality become better for higher energy.

Results

Measured Molière radius

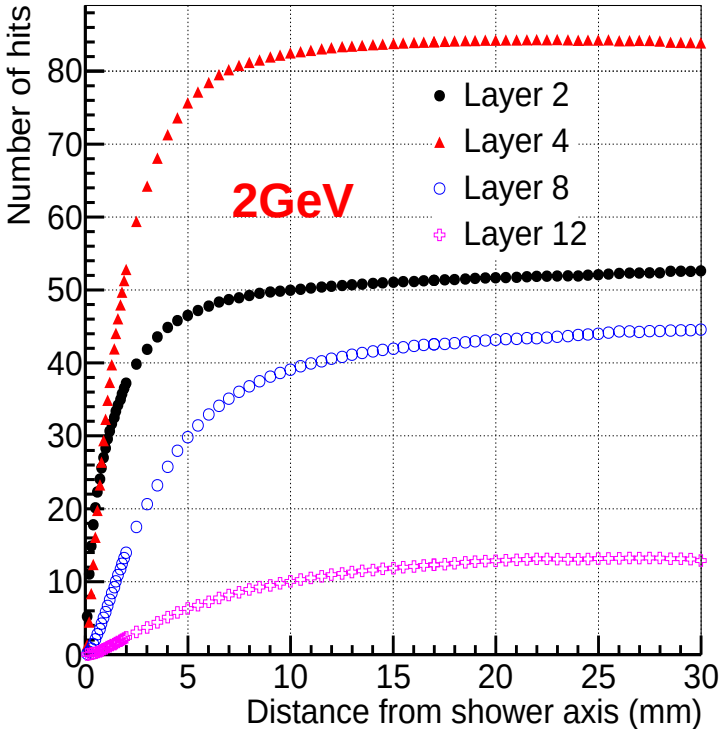

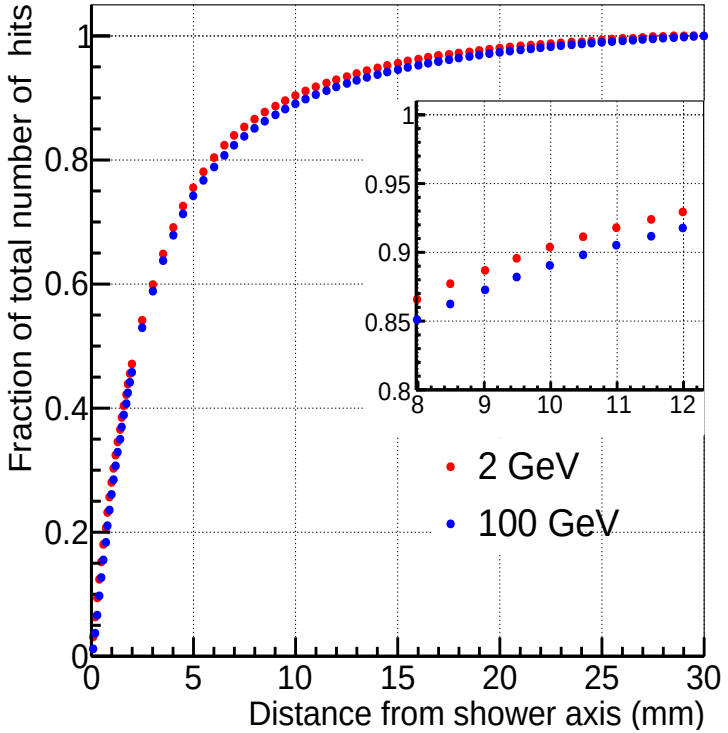

$$\frac{\sum_{l=0}^{23}\int_0^{R_M} 2\pi r\rho_l(r)dr}{\sum_{l=0}^{23}\int_0^{R_{\rm tot}} 2\pi r\rho_l(r)dr} = 90\%$$

- R=25 mm should be sufficient for shower containment.
- Discrepancy between low and high energy may due to saturation at small r.

Results

Shower profile comparison

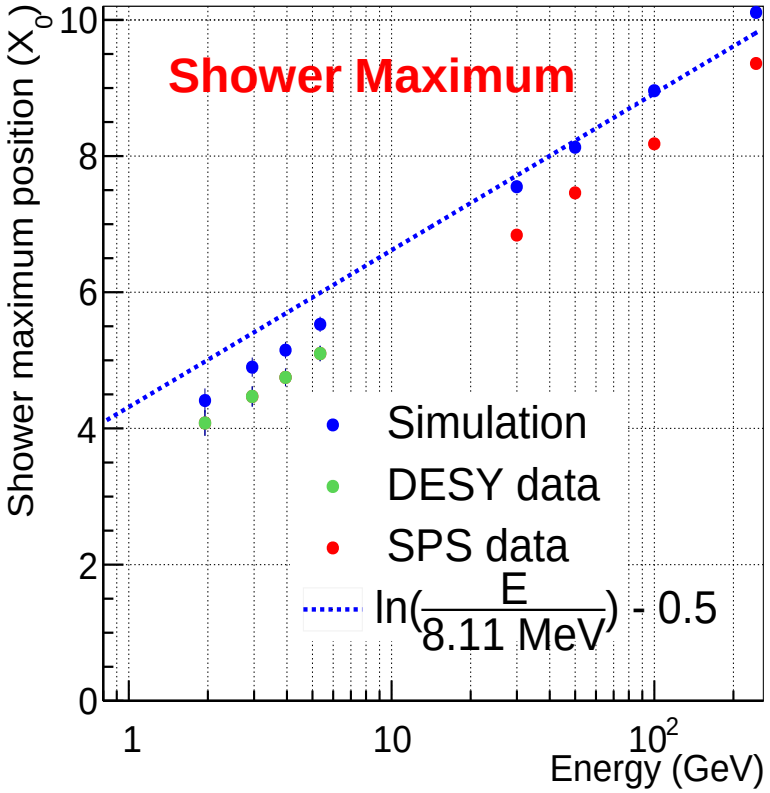

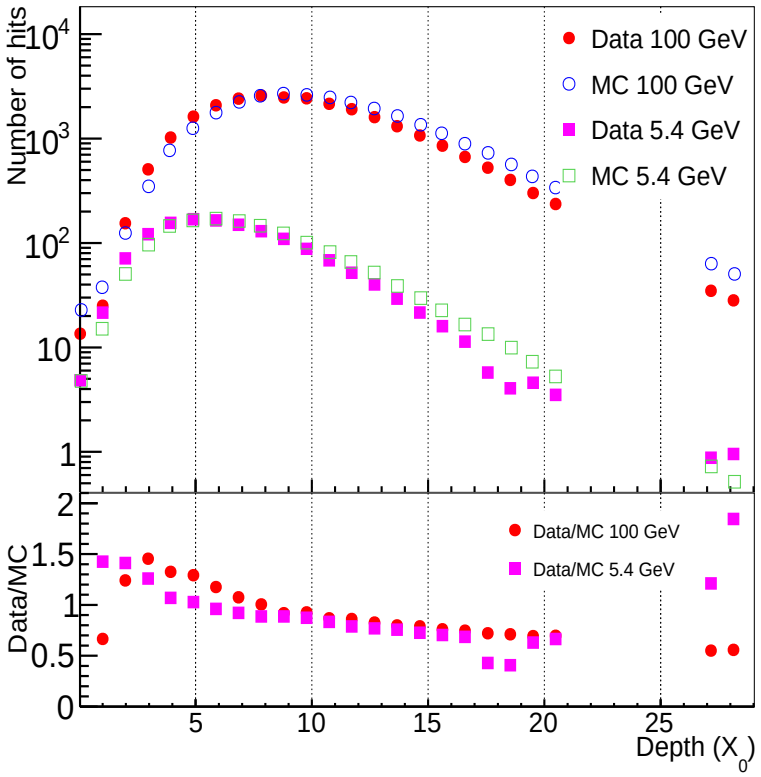

Possible reasons:

- Empirical equation is for homogeneous calorimeter.
- Additional material, e.g. the air, scintillators, window of beam pipe…??
- Not complete adequate description of the model in GEANT?

Two-Shower Separation

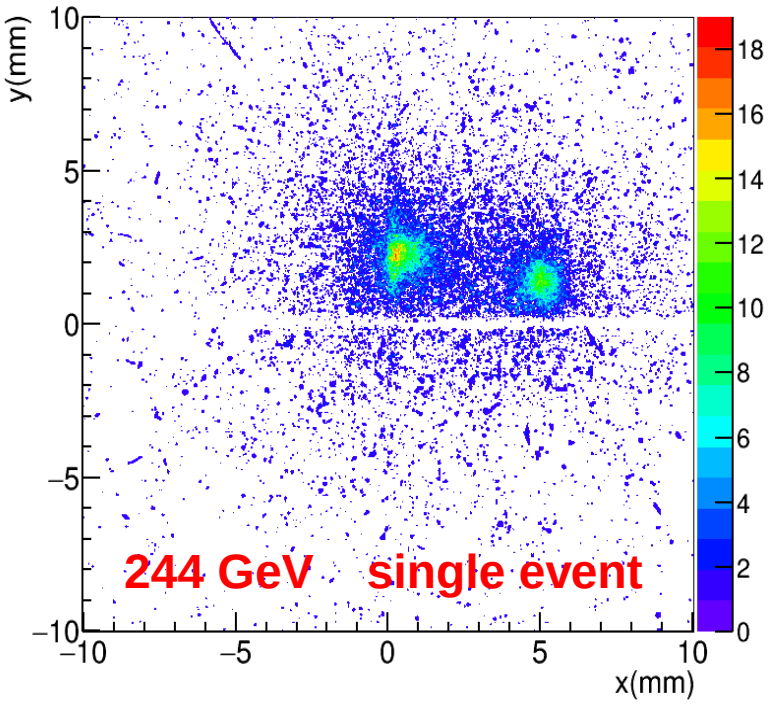

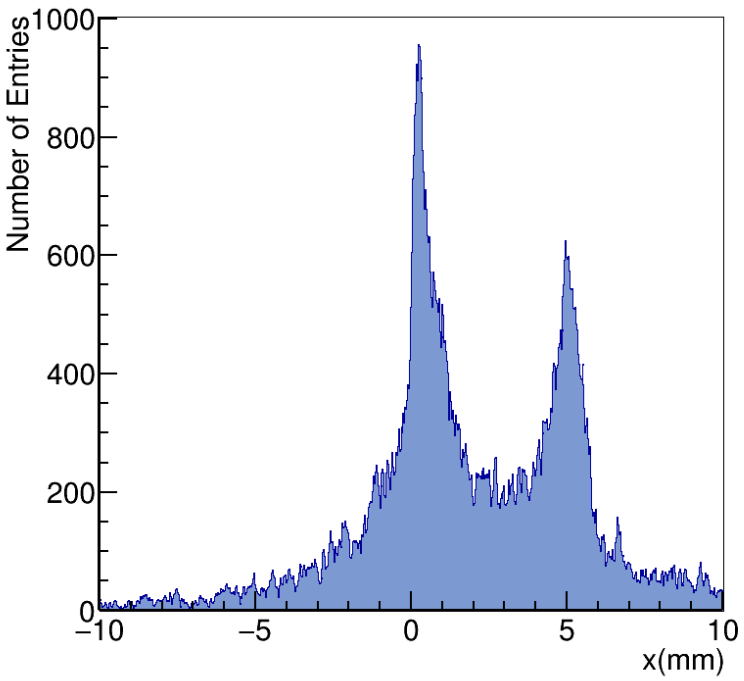

- Good separation power of two close showers down to few mm

Other Application

Other Application

What are we measuring in traditional CT?

- Measure linear attenuation coefficient μ when x-ray penetrates the phantom(human body).
- Attenuation coefficient is a measure of how rapidly x-rays are absorbed within the materials.
- The 2-D/3-D images can be reconstructed by algorithm(FBP, Iterative).

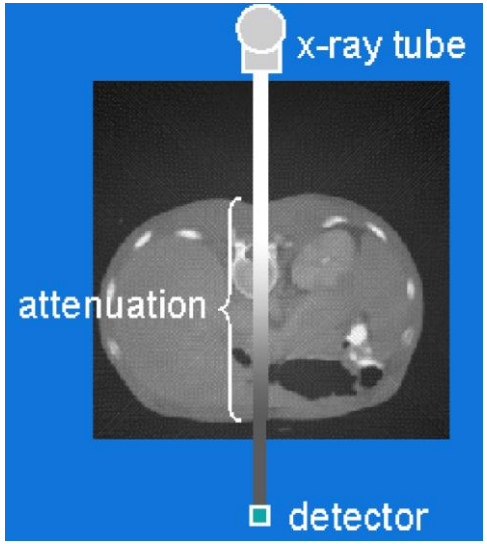

$$c_{CT} = \mathrm{k}\frac{\mu - \mu_w}{\mu_w}$$ Unit in **Hu**, k=1000

	Water	Bone	Air
μ	1.0	2.0	0
C_{CT}	0	1000	-1000

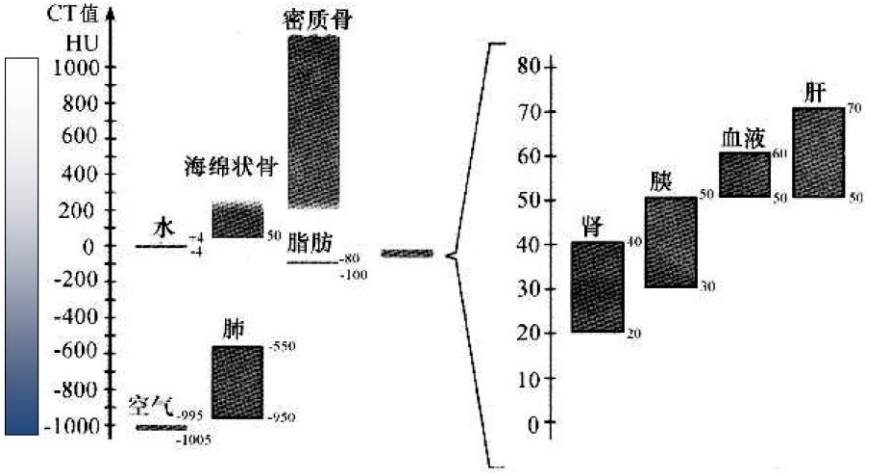

Other Application

Proton CT

A.G. Santos, CALICE meeting 2019, Utrecht

Proton therapy at present:

CT Hounsfield Units (HU) → Calibration curve → Relative Stopping power (RSP) → Dose calculation → Treatment planning

Uncertainties !!

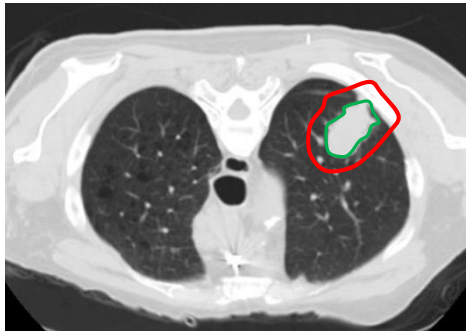

Problems

- Conversion of range uncertainties : 3-5%(head, spine)
- Improvement→ Dual Energy CT: ~ 2%
- However, CT artifact→ inaccurate RSP map

Safety margins at different proton therapy centers

Institution	Relative margin	Fixed margin	At 20 cm depth
University of Florida Proton Therapy Institute	2.5%	1.5 mm	6.5 mm
Massachusetts General Hospital	3.5%	1 mm	8 mm
MD Anderson Proton Therapy Center	3.5%	3 mm	10 mm
Loma Linda University Medical Center	3.5%	3 mm	10 mm
Roberts Proton Therapy Center	3.5%	3 mm	10 mm

Proton CT

- Direct RSP maps
- No artifacts
- Reduction of imaging dose compare to CT.

Reduction of treatment margins

Other Application

Proton CT

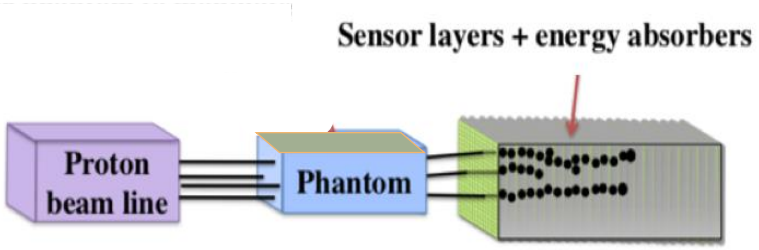

Option 1

H.E.S. Pettersen, et.al. NIMA, 860 (2017) 51-61

- HG Calorimeter to measure residual range/energy.
- Easy to implement.
- Requires high precision tracking algorithm.
- Multiple coulomb scattering may degrade the image quality.

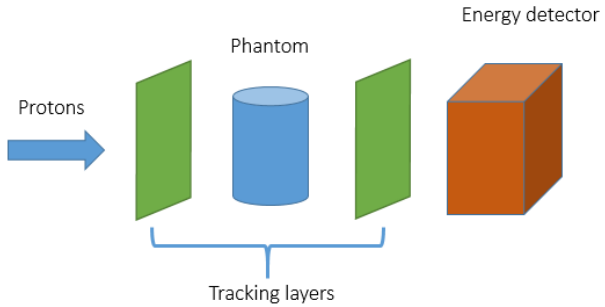

Option 2

Funded by China Postdoctoral Science Foundation

- Position sensitive layers to track protons.(MAPS)
- Energy detector to measure residual energy.(calorimeter)
- Reconstruct scattering point in the phantom to improve the quality of the imaging (requires algorithm).

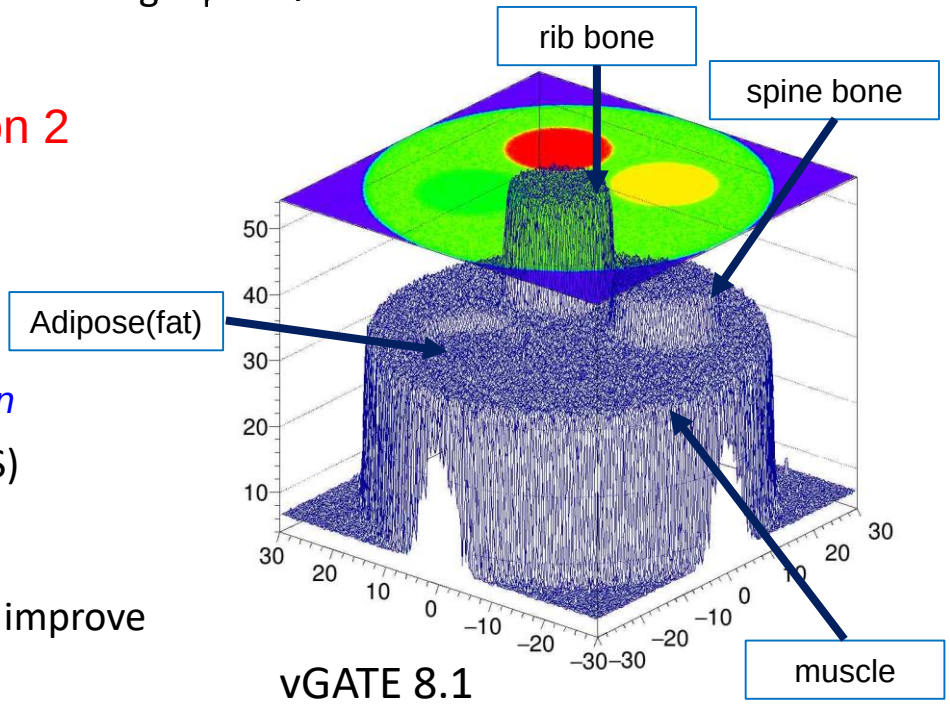

Conclusions

- **Successful Proof of Principle of Particle Counting Calorimetry.**
  - A high granularity digital Si-W calorimeter prototype for FoCal has been built and tested.
  - Good linearity has been achieved.
  - General performance agrees well with the simulation.
- **Spatial granularity allows unique measurements**
  - High resolution lateral shower profiles have been obtained.
  - Very efficient two-shower separation should be possible.
  - Excellent position resolution allows to be used in other domains, e.g. **pCT**.

Thank you!

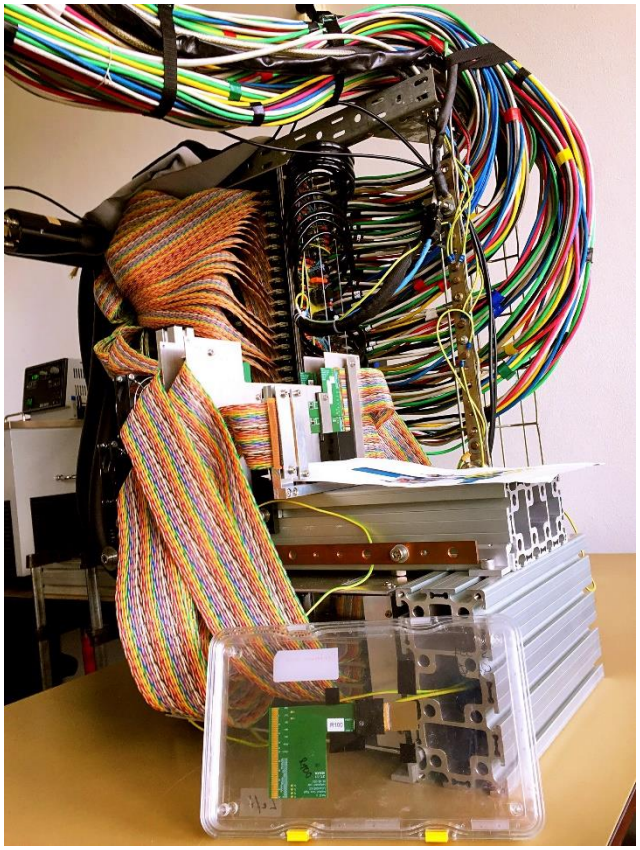

References:

FoCal related publications

1. *JINST 8 (2013) P03015*
2. *JINST 13 (2018) P01014*
3. *NIMA, 860 (2017) 51-61*

FoCal related PhD theses

1. *M. Reicher, "Digital Calorimeter using Pixel Sensors", 2016*
2. *C. Zhang, "Measurements with a High-Granularity Digital Electromagnetic Calorimeter ", 2017*
3. *H. Wang, "Prototype Studies and Simulations for a Forward Si-W Calorimeter at the LHC", 2018*

Back up

Introduction

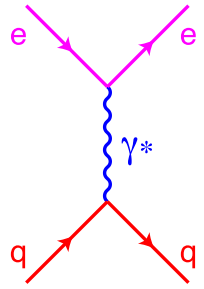

DIS (LO)

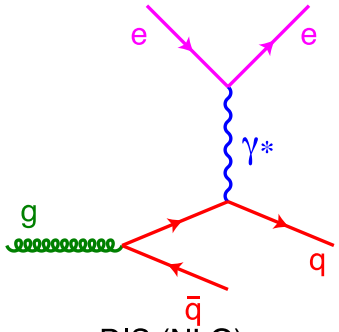

DIS (NLO)

Direct photons produce from parton interaction can provide strong constraints on the gluon PDFs.

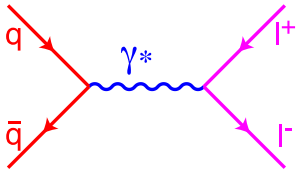

DY (LO)

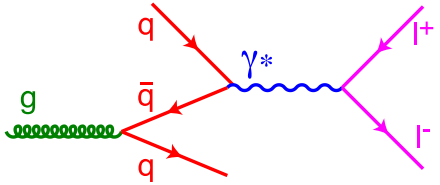

DY, virtual Compton (NLO)

PDF of parton can be constrained by a coincidence measurement.

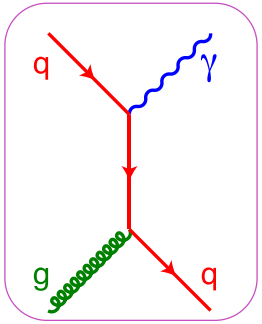

direct-γ, Compton (LO)

Examples of Feynman diagrams for electromagnetic processes relevant for probing the parton distribution functions

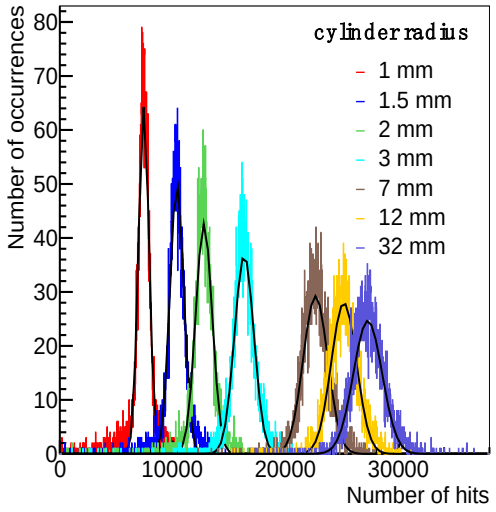

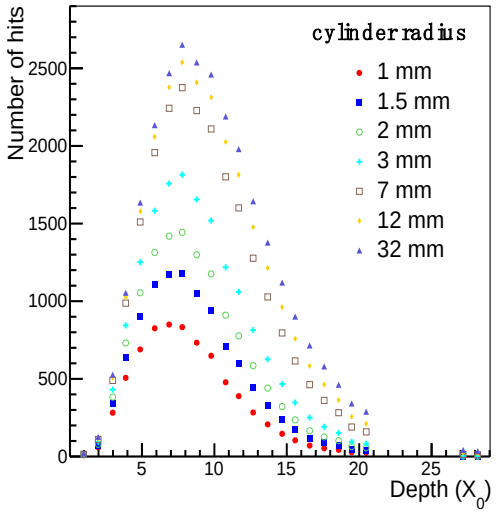

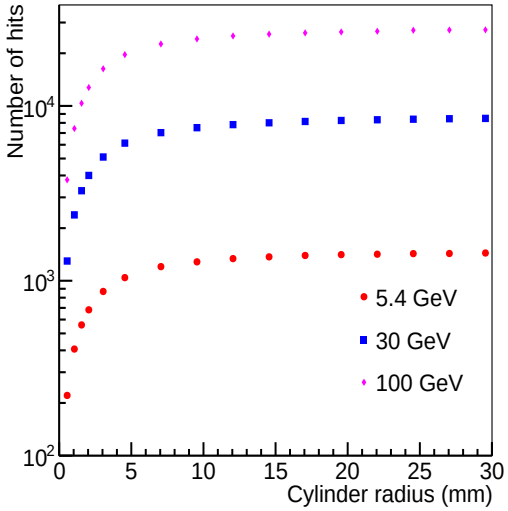

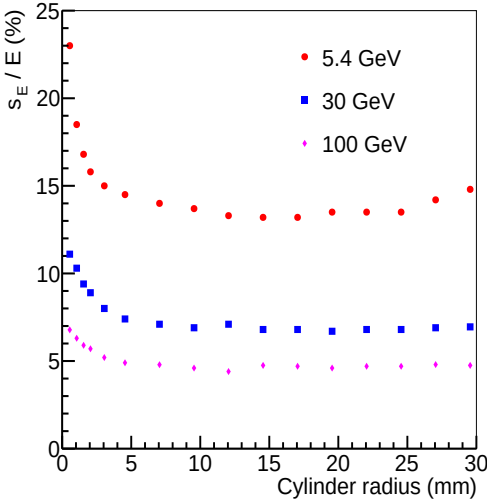

100 GeV

Detector properties as a function of cylinder radius

Test Beam Data Analysis

Single event

Single layers pixel map

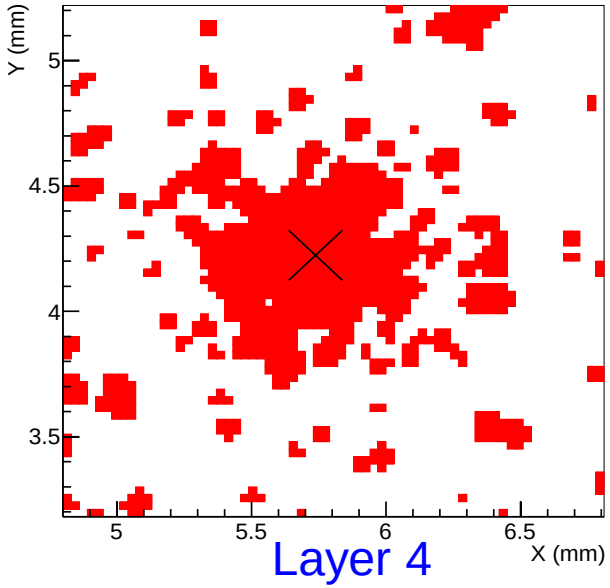

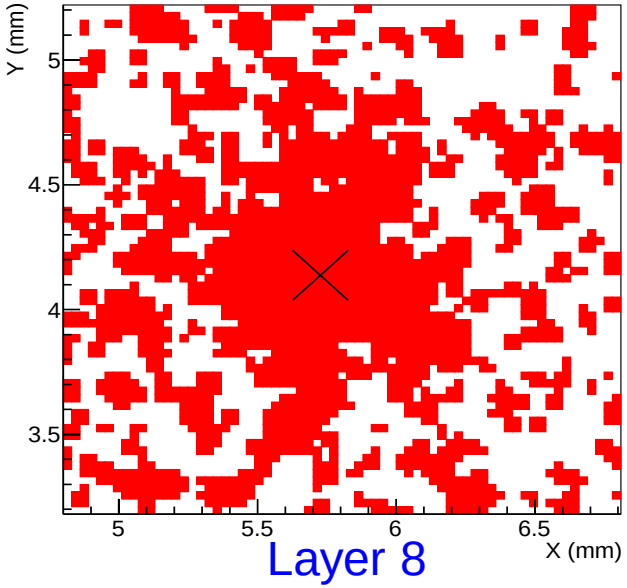

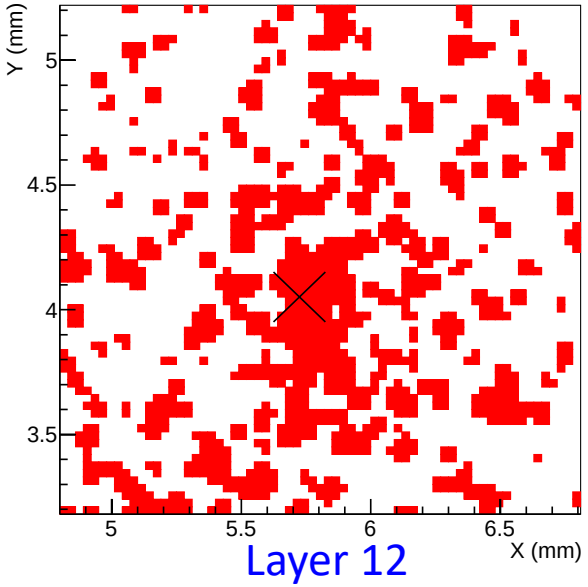

Tuning of Sensors Thresholds

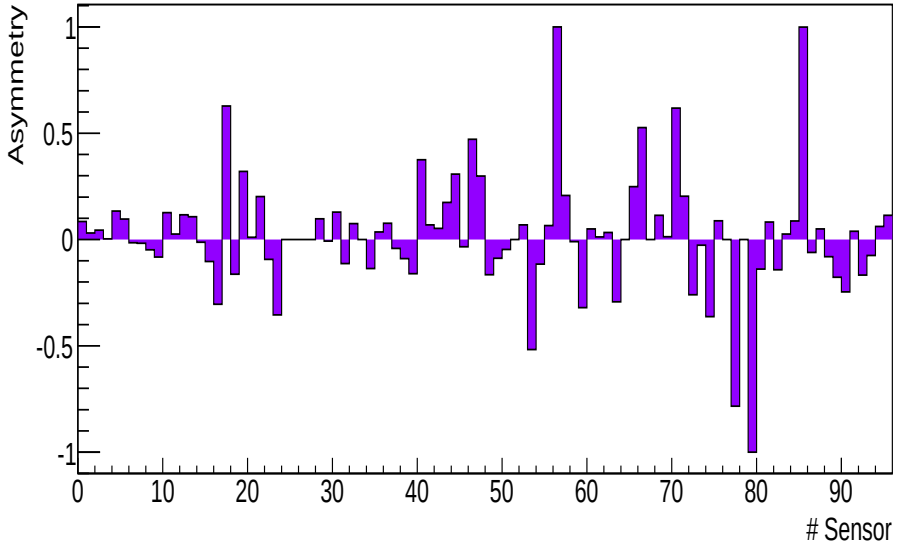

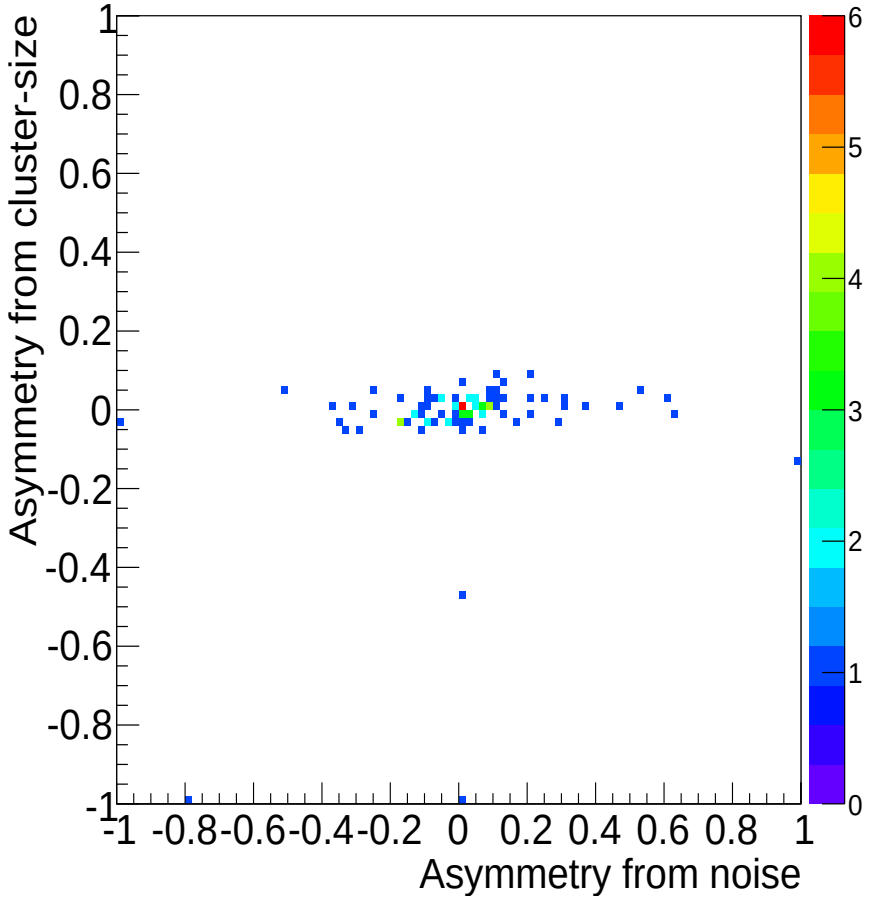

Design

Measured sensor efficiency

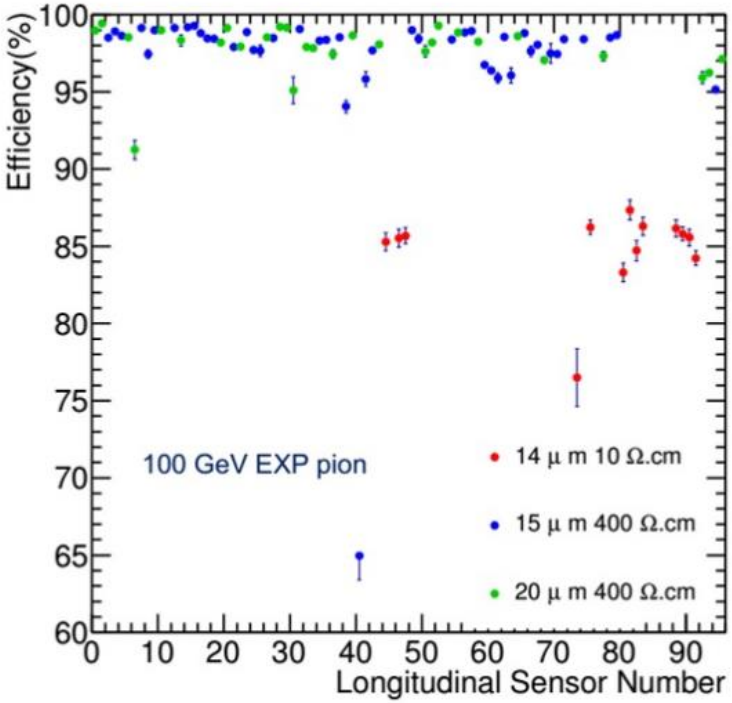

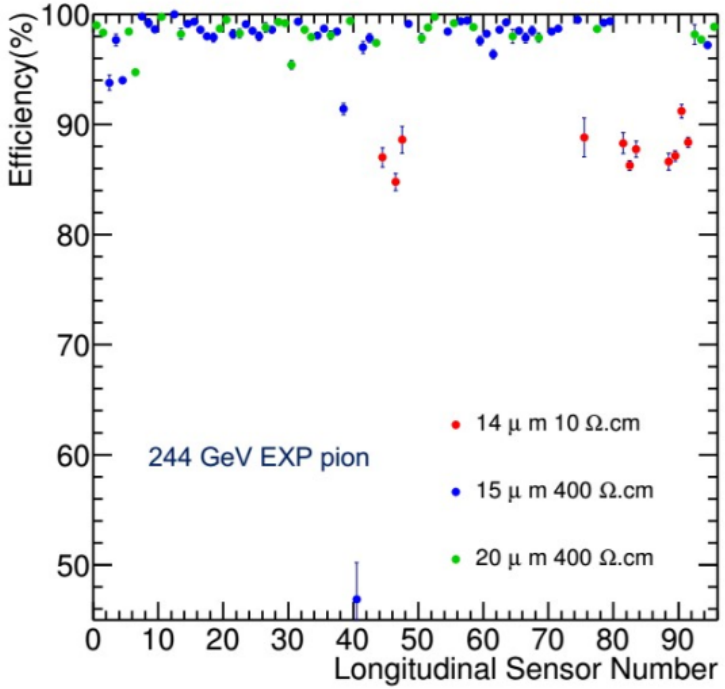

- Use pions instead of muons.
- Gap and overlap region are not taken into account
- Remove secondary tracks by project tack length in 2-D.

$$\epsilon_l^q = \frac{N_{assoc}}{N_{total}}$$

Relatively good detection efficiency
Significant different sensitivity for different types of sensors

Data Quality

Noise

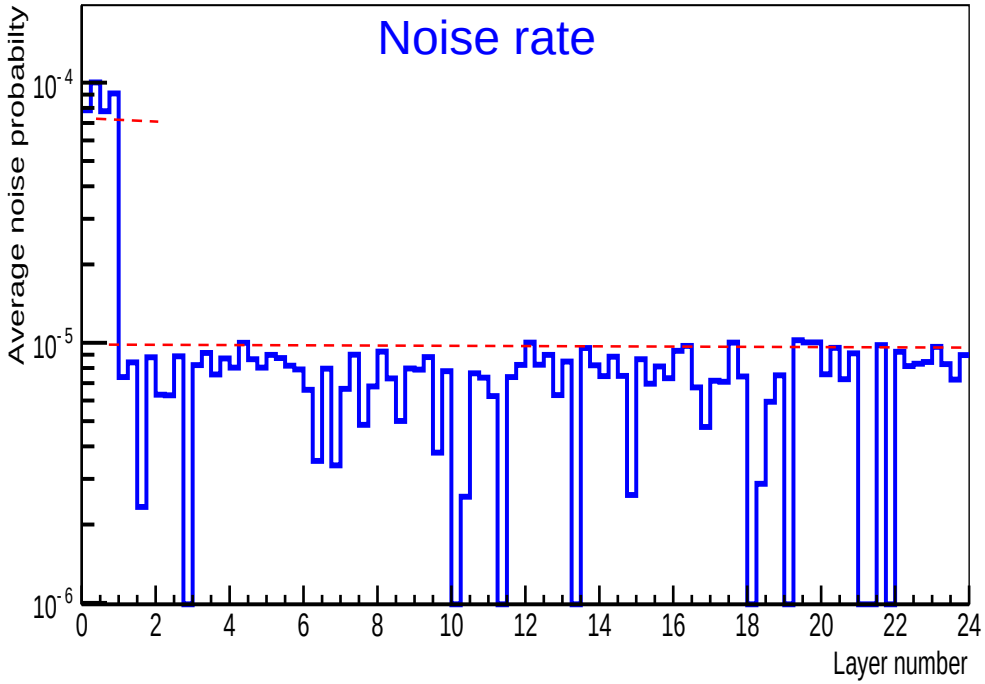

Noise spectrum

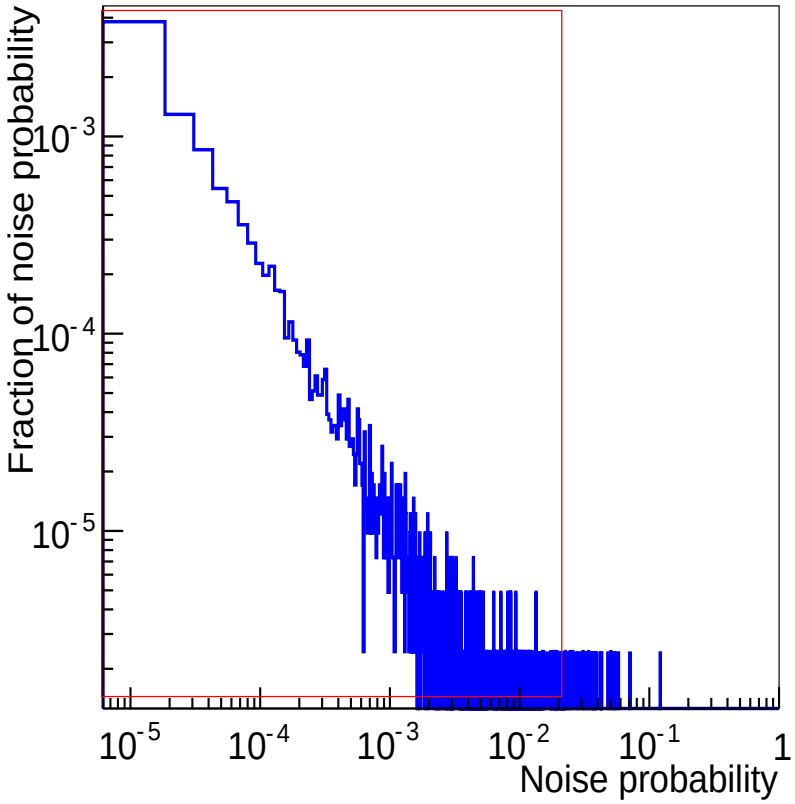

Due to faulty channels and hot pixels are removed, the average noise rate of working pixels is lower than 10^{-5} for most of the sensors.

So a better way of tuning the threshold is to tune to obtain similar noise spectrum.

Data Quality

Map of hits distribution

Cleaned Data

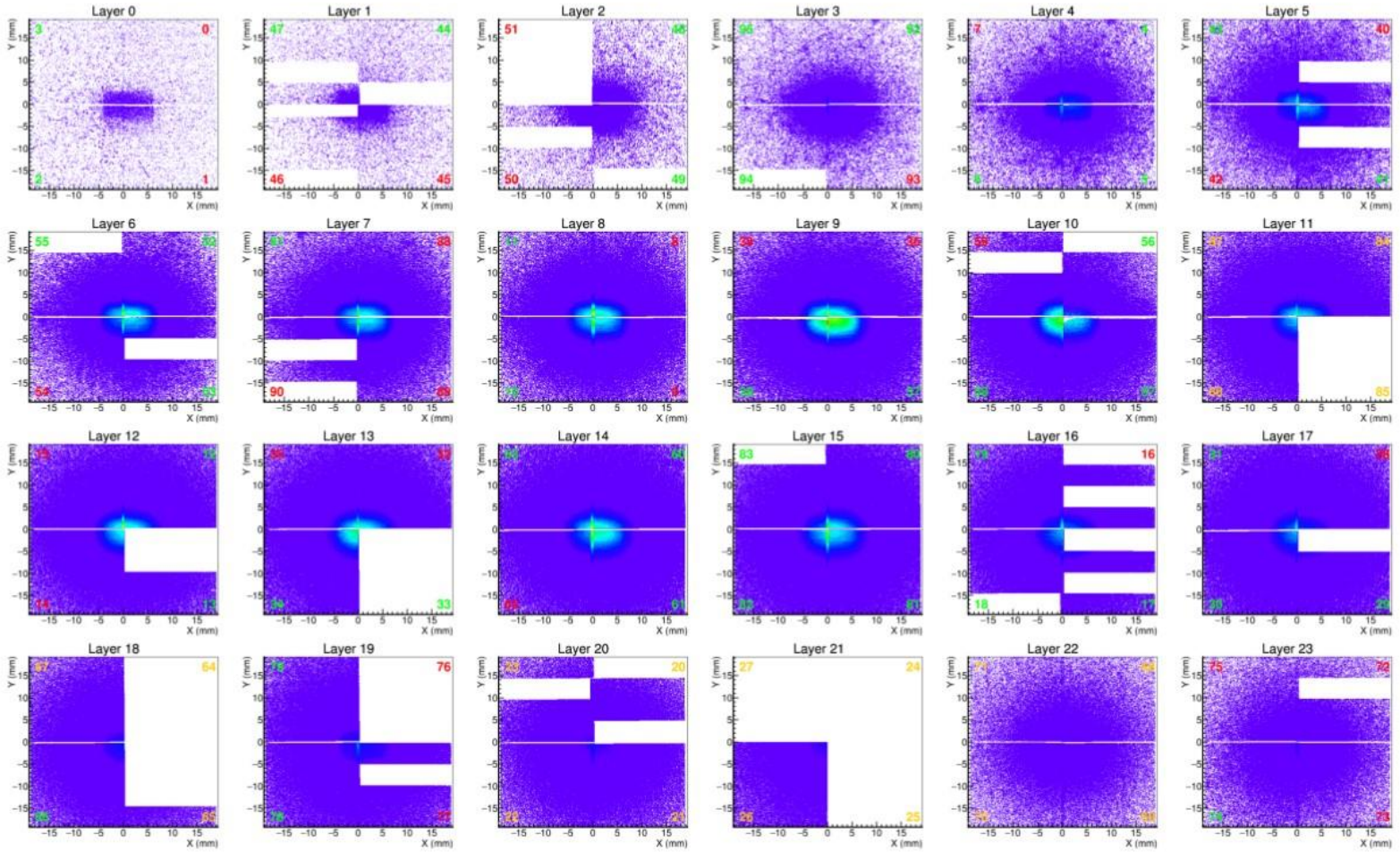

Test Beam Data Analysis

Calibration quality

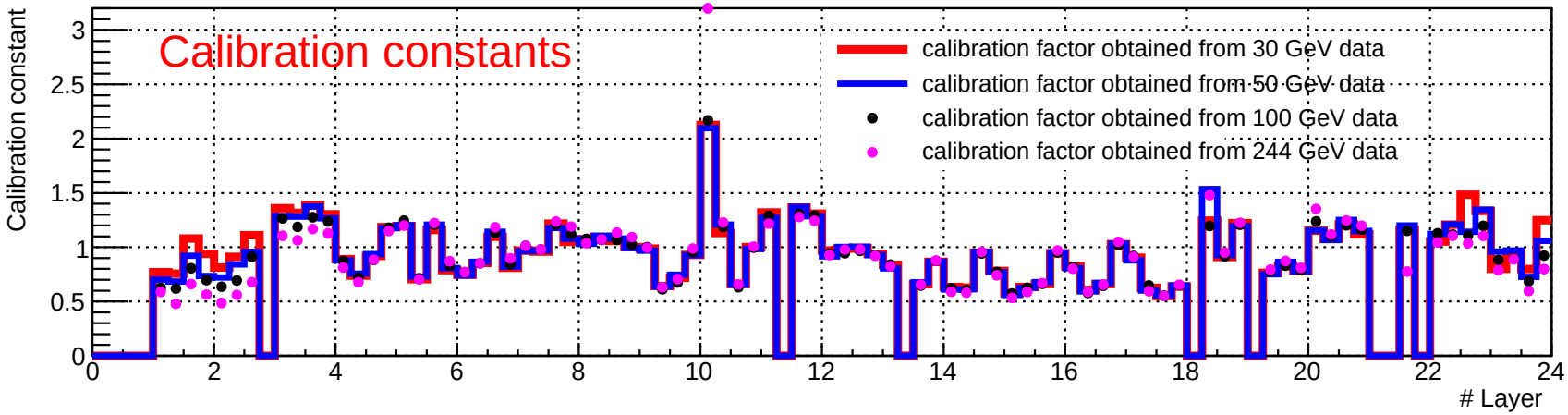

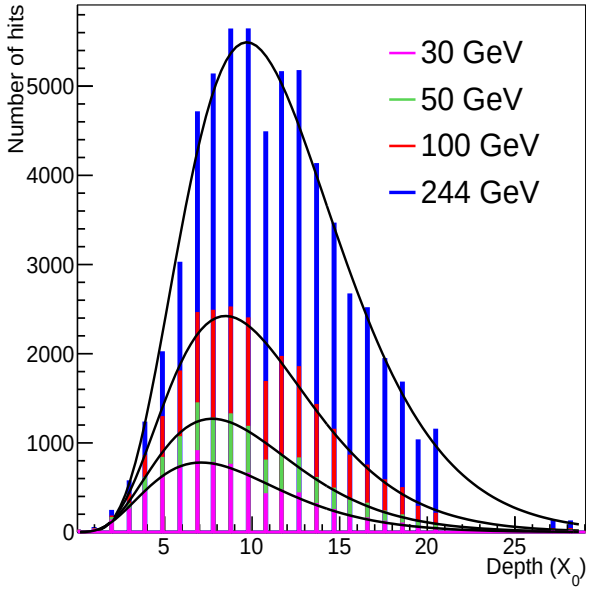

Longitudinal profiles with Gamma function fit curve.

Test Beam Data Analysis

Calibration quality

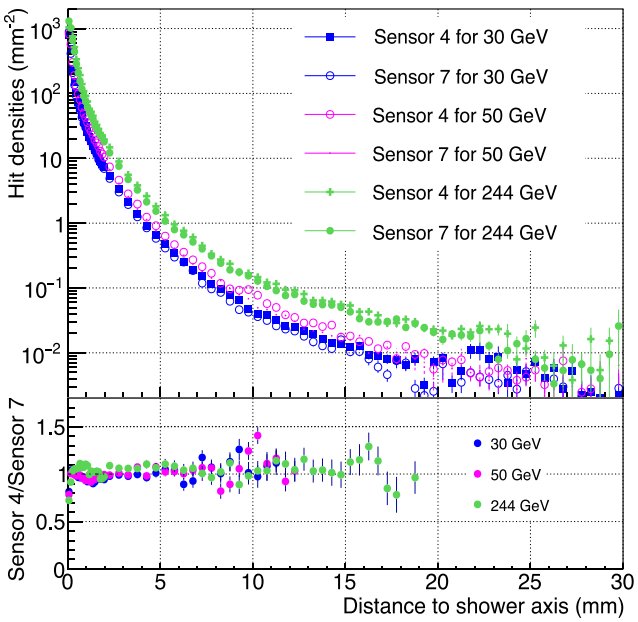

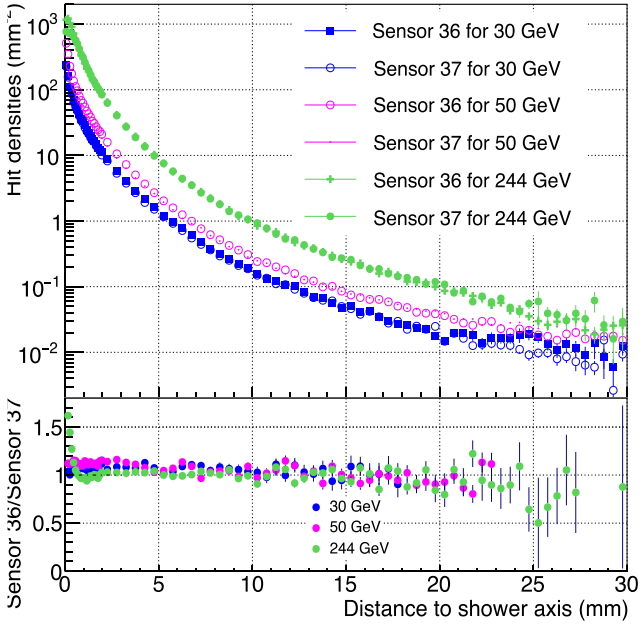

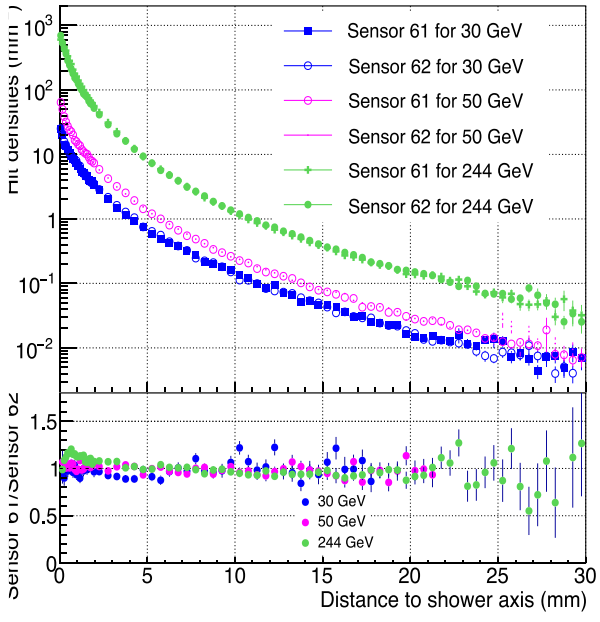

sensors 4, 37, 61 and 66: 15 m thick with 400 /cm;
sensors 7, 36 and 62: 20 m thick with 400 /cm;
sensors 67: 14 m thick with 10 /cm.

Correlation between calibration constants and cluster size

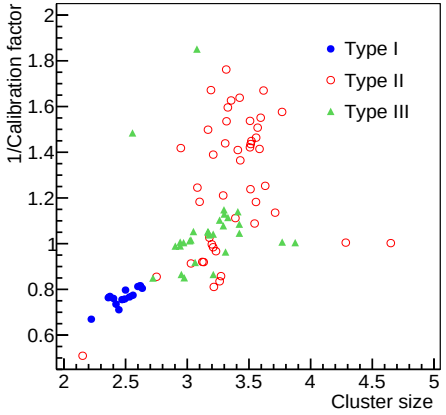

Results

Detector response

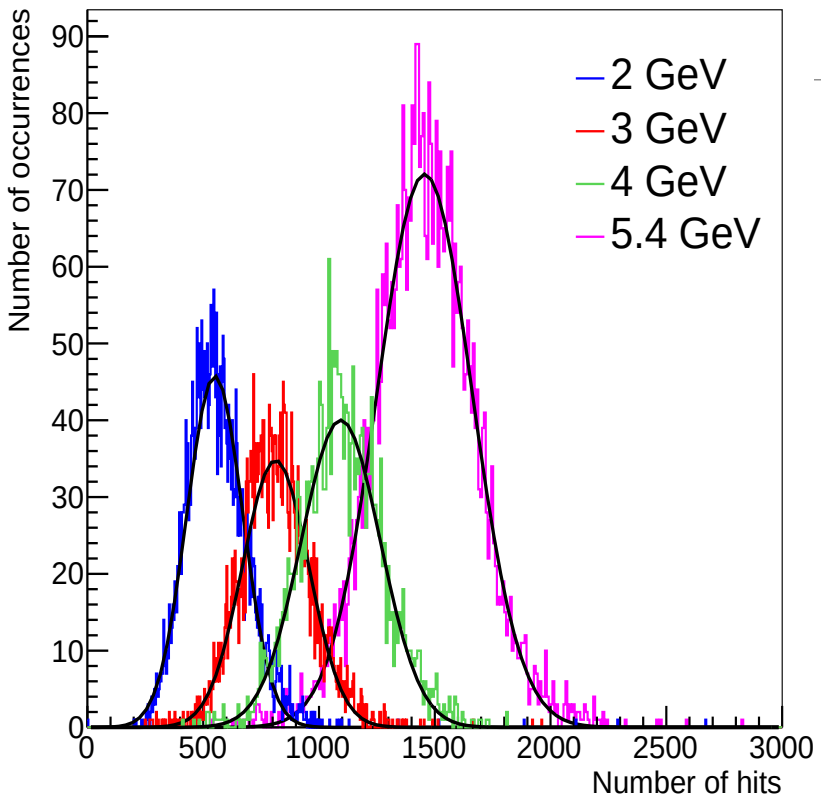

DESY

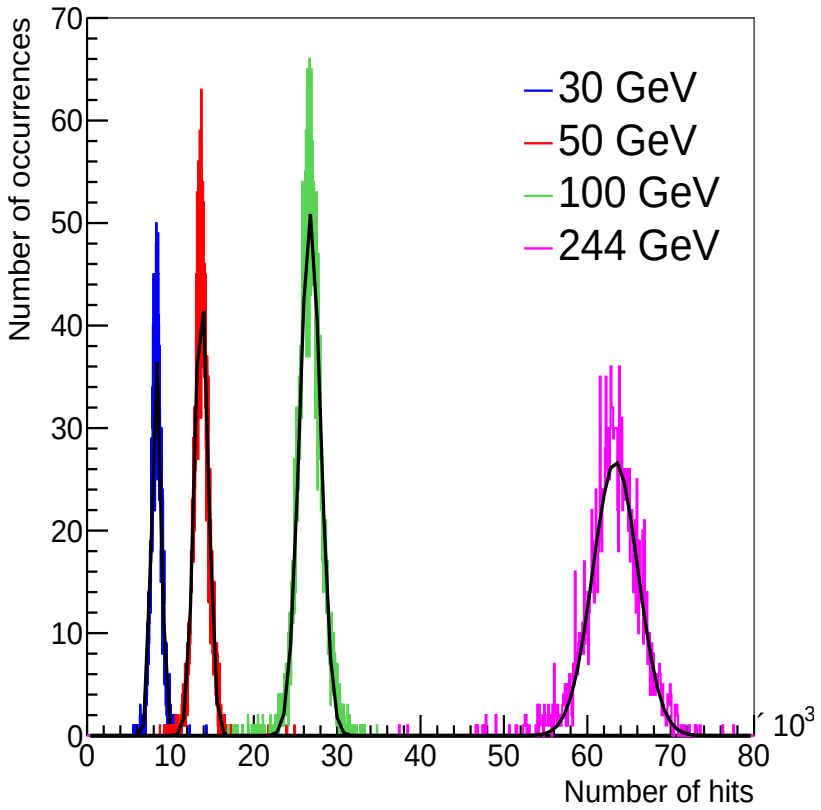

SPS

Simulation

Effects of charge diffusion

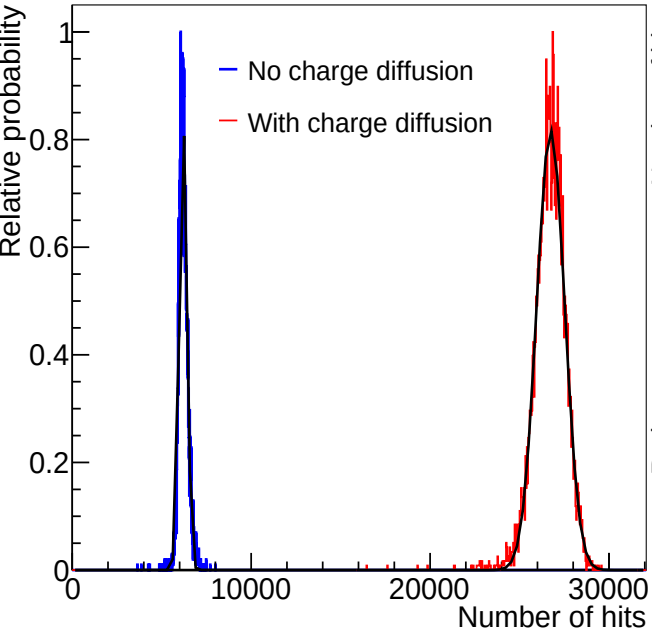

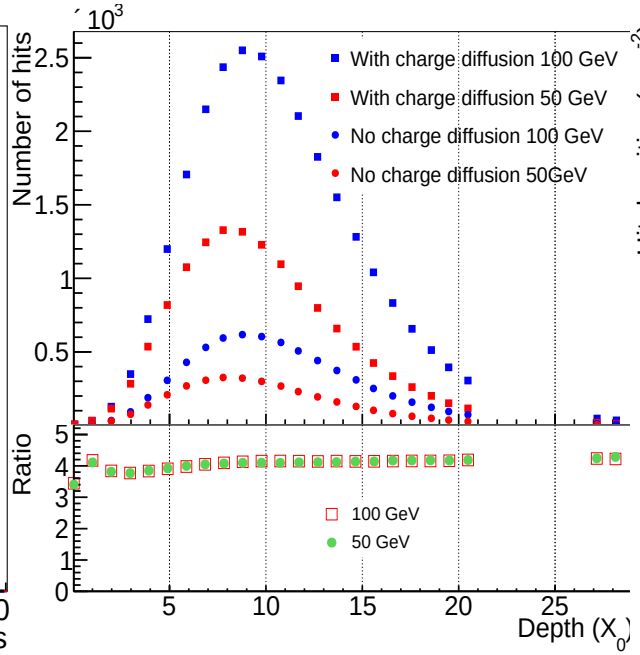

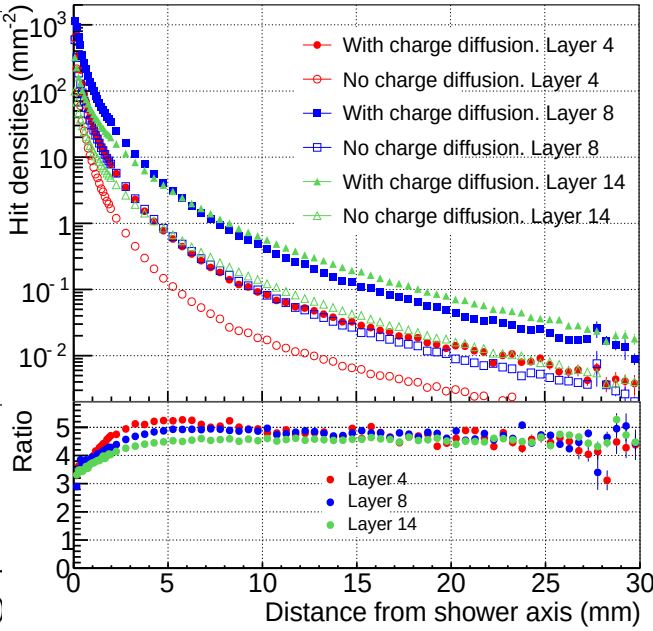

The total effective gain factor is determined by

- an interplay of charge sharing.
- energy deposition.
- the angle of the particles relative to the sensor.

Very close to the shower core, the gain factor is smaller than the average due to saturation.

Fitting the longitudinal profiles

Gamma function fits to longitudinal profiles with and without charge diffusion

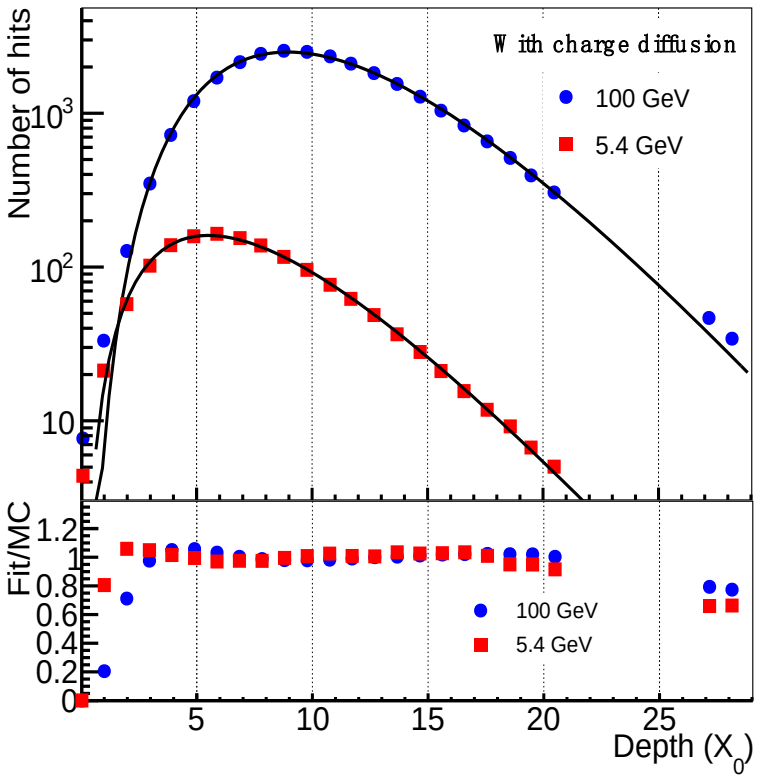

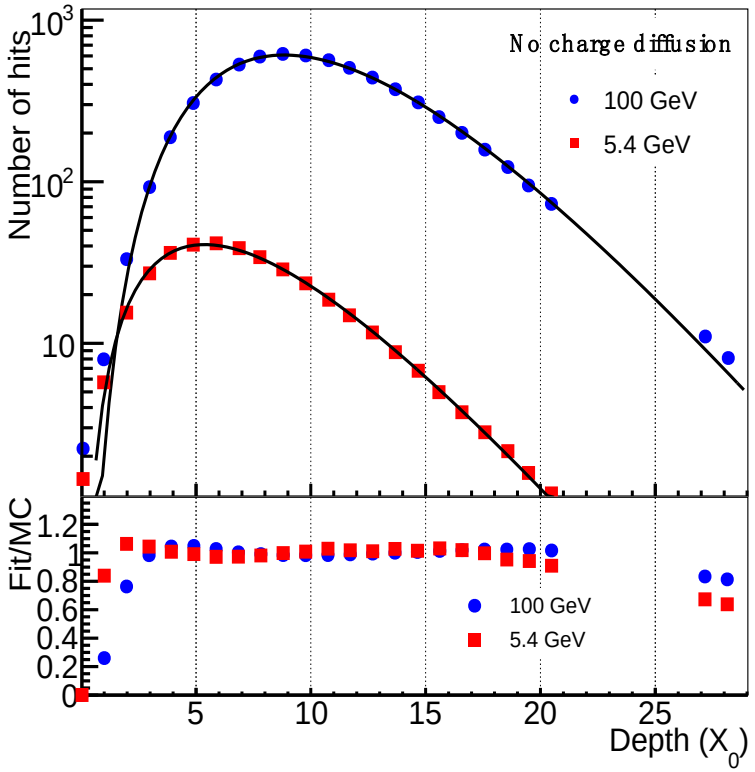

The Gamma function does not well describe the first 2-3 radiation lengths and the last 2 radiation lengths.

ALIPID sensor charistics

- Monolithic Active Pixel Sensor
- Chip size: 30.00 mm x 15.00 mm
- Pixel matrix: 1024 x 512 (=524288 pixels / chip)
- Active area: 29.94 mm x 13.76 mm
- Pixel size: 29.24 µm x 26.88 µm
- Hit driven readout
- Readout speed: 400 Mb/s - 1.2 Gb/s
- Power consumption proportional to the occupancy.

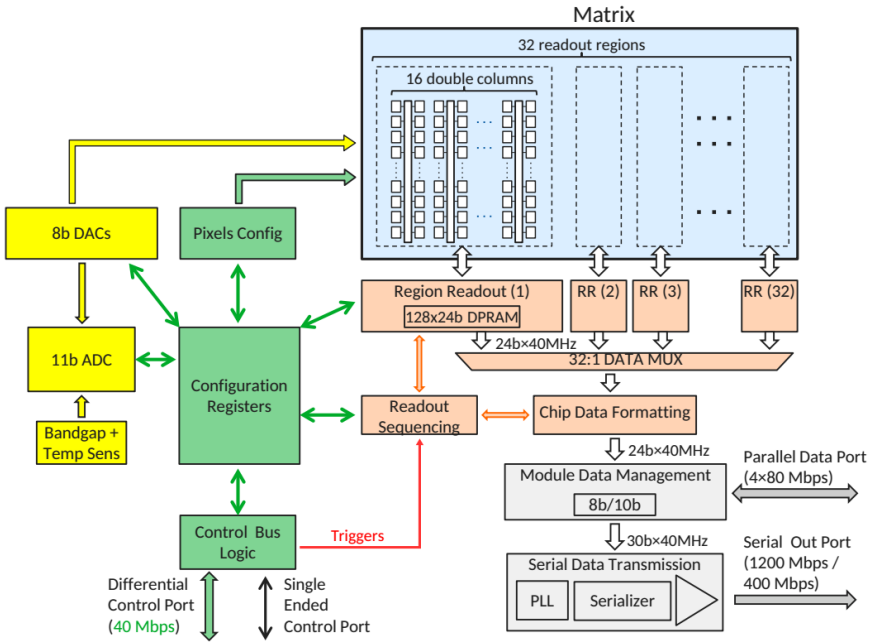

Results

Shower position resolution

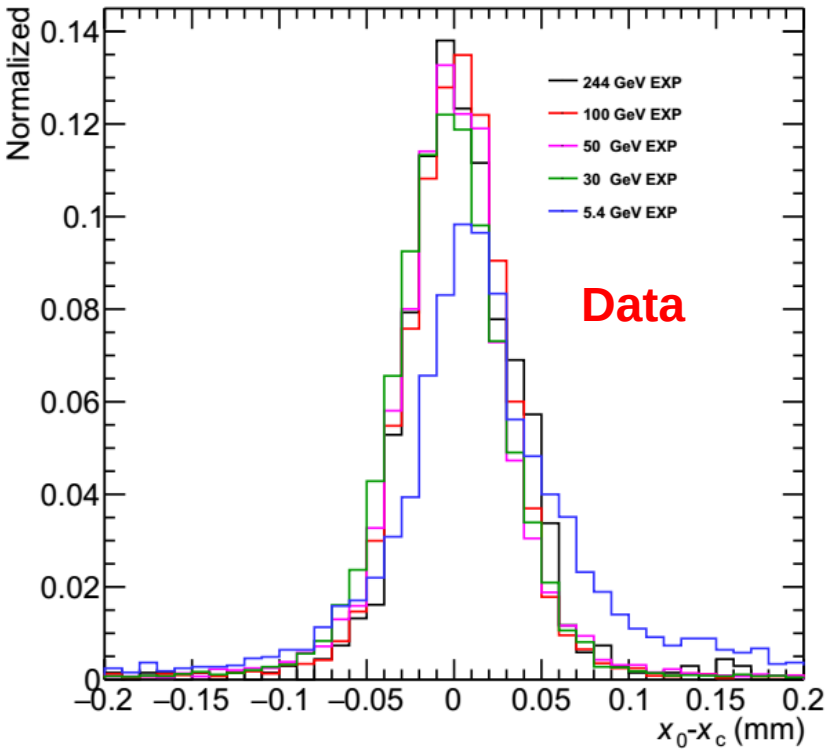

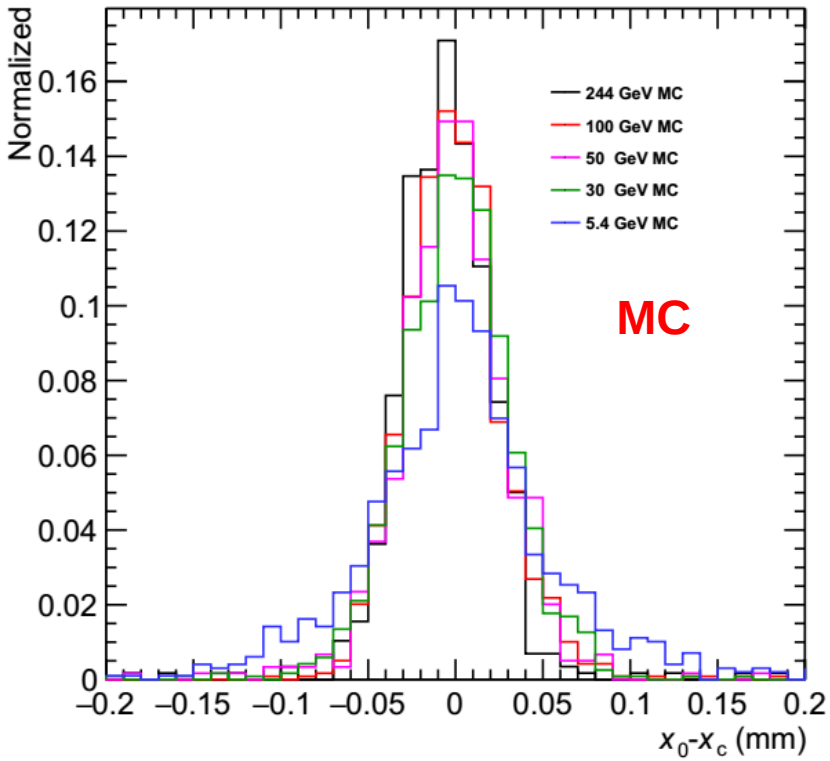

X_0: reconstructed shower center

X_c: cluster found in the first layer

- Very good agreement between Data and MC.
- Beam inclination can be removed successfully.

Results

Shower profile comparison

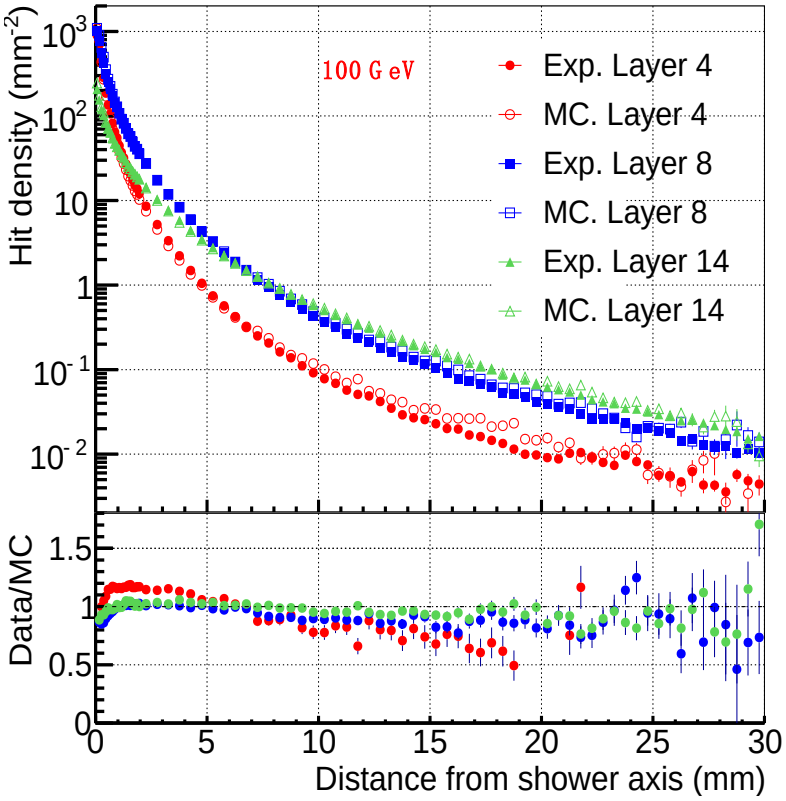

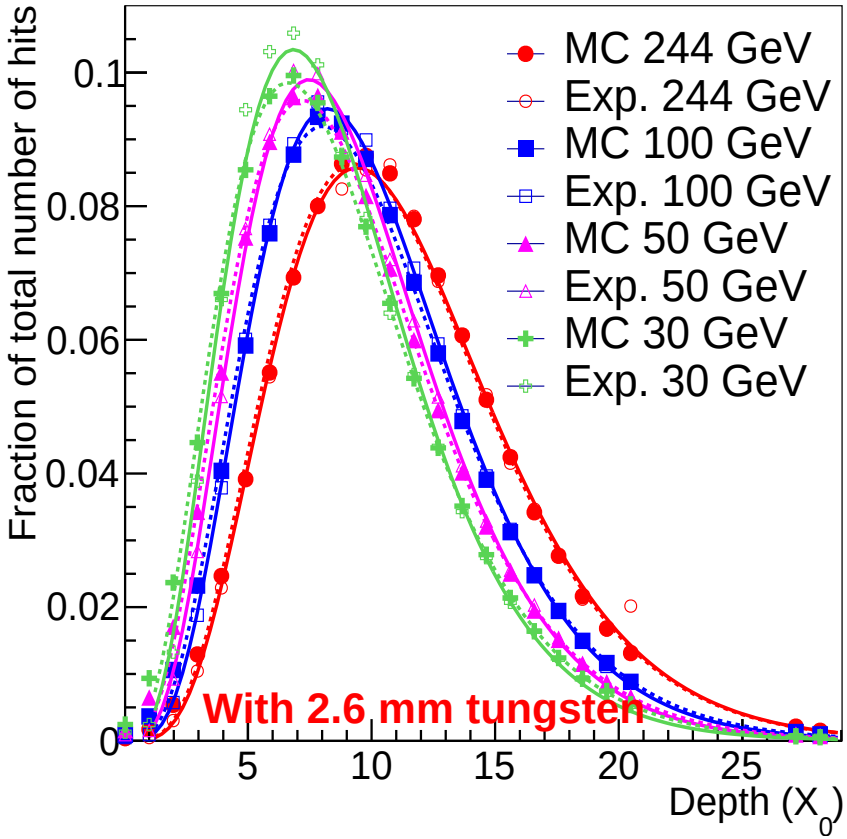

- Left: Comparison of lateral profiles between data and simulation, the lower panels show the ratio of data to simulation.
- Right: Longitudinal profile when a 2.6 mm tungsten is placed in front of the detector.

Outlooks

Two-shower separation

- Shower centre position calculation
- Energy reconstruction
- Shower shape decomposition

Some effects

- Dead sensors and channels.
- Gap and overlap regions.
- Saturation, charge diffusion and charge sharing -> measurements of response, Moliere radius.
- Leakage, particle angle with silicon -> Moliere radius.